③

AFGL-TR-88-0295

Ion and Electron Interactions at Thermal
and Suprathermal Energies

David Smith
Nigel G. Adams
Charles R. Herd

AD-A201 418

University of Birmingham
Department of Space Research
Birmingham, B15 2TT, UNITED KINGDOM

30 September 1988

Scientific Report No. 1

DTIC
S **ELECTE**
D
OCT 2 5 1988

AIR FORCE GEOPHYSICS LABORATORY
AIR FORCE SYSTEMS COMMAND
UNITED STATES AIR FORCE
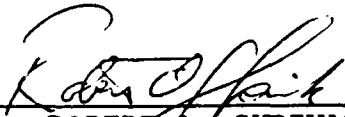HANSCOM AIR FORCE BASE, MASSACHUSETTS 01731-5000

88 1024 090

"This technical report has been reviewed and is approved for publication"

_____
JOHN F. PAULSON
Contract Manager

_____
JOHN E. RASMUSSEN
Branch Chief

FOR THE COMMANDER

_____
ROBERT A. SKRIVANEK
Division Director

This report has been reviewed by the ESD Public Affairs Office (PA) and is releasable to the National Technical Information Service (NTIS).

Qualified requestors may obtain additional copies from the Defense Technical Information Center. All others should apply to the National Technical Information Service.

If your address has changed, or if you wish to be removed from the mailing list, or if the addressee is no longer employed by your organization, please notify AFGL/DAA, Hanscom AFB, MA 01731-5000. This will assist us in maintaining a current mailing list.

Do not return copies of this report unless contractual obligations or notices on a specific document requires that it be returned.

REPORT DOCUMENTATION PAGE

Form Approved
OMB No. 0704-0188

1a. REPORT SECURITY CLASSIFICATION	1b. RESTRICTIVE MARKINGS
Unclassified	

2a. SECURITY CLASSIFICATION AUTHORITY	3. DISTRIBUTION/AVAILABILITY OF REPORT
	Approved for public release;
2b. DECLASSIFICATION/DOWNGRADING SCHEDULE	Distribution unlimited

4. PERFORMING ORGANIZATION REPORT NUMBER(S)	5. MONITORING ORGANIZATION REPORT NUMBER(S)
	AFGL-TR-88-0295

6a. NAME OF PERFORMING ORGANIZATION	6b. OFFICE SYMBOL (If applicable)	7a. NAME OF MONITORING ORGANIZATION
University of Birmingham		European Office of Aerospace Research and Development

6c. ADDRESS (City, State, and ZIP Code)	7b. ADDRESS (City, State, and ZIP Code)
Department of Space Research P.O. Box 363 Birmingham B15 2TT, UNITED KINGDOM	223/231 Old Marylebone Road London NW1 5th, UNITED KINGDOM

8a. NAME OF FUNDING/SPONSORING ORGANIZATION	8b. OFFICE SYMBOL (If applicable)	9. PROCUREMENT INSTRUMENT IDENTIFICATION NUMBER
Air Force Geophysics Laboratory		AFOSR-87-0355

8c. ADDRESS (City, State, and ZIP Code)
Hanscom AFB
Massachusetts 01731-5000

10. SOURCE OF FUNDING NUMBERS			
PROGRAM ELEMENT NO.	PROJECT NO.	TASK NO.	WORK UNIT ACCESSION NO.
62101F	2303	G1	AJ

11. TITLE (Include Security Classification)
Ion and Electron Interactions at Thermal and Suprathermal Energies

12. PERSONAL AUTHOR(S)
David Smith, Nigel G. Adams, Charles R. Herd

13a. TYPE OF REPORT	13b. TIME COVERED	14. DATE OF REPORT (Year, Month, Day)	15. PAGE COUNT
Scientific Report #1	FROM _____ TO _____	1988 September 30	

16. SUPPLEMENTARY NOTATION

17. COSATI CODES			18. SUBJECT TERMS (Continue on reverse if necessary and identify by block number)
FIELD	GROUP	SUB-GROUP	Electron attachment, Flowing afterglow/Langmuir probe, Selected ion flow drift tube.
			Dissociative recombination,
			Ion-molecule reactions,

19. ABSTRACT (Continue on reverse if necessary and identify by block number)

The flowing afterglow/Langmuir probe (FALP) and the selected ion flow drift tube (SIFDT) apparatuses have been used to study (i) dissociative electron attachment reactions of several organo-halogen molecules, including the unstable radical species CCl_3 and CCl_2Br (ii) dissociative recombination reactions of several polyatomic positive ions, and preliminary data on the neutral products of several such reactions are reported (iii) the proton affinities of several molecular species and the collisional breakup of $C_2H_5OH_2^+$ ions.

20. DISTRIBUTION/AVAILABILITY OF ABSTRACT	21. ABSTRACT SECURITY CLASSIFICATION
☐ UNCLASSIFIED/UNLIMITED ☐ SAME AS RPT. ☐ DTIC USERS	Unclassified

22a. NAME OF RESPONSIBLE INDIVIDUAL	22b. TELEPHONE (Include Area Code)	22c. OFFICE SYMBOL
John Paulson		AFGL/LID

DD Form 1473, JUN 86   Previous editions are obsolete.   SECURITY CLASSIFICATION OF THIS PAGE

C O N T E N T S

PREFACE

PREFACE

This work is part of a larger programme of ionic reaction studies at thermal energies conducted by the senior authors of this report. The overall programme includes studies of ion/neutral reactions, electron attachment, electron/ion recombination, ion/ion recombination, and other plasma reaction processes. The work is largely intended as a contribution to the physics and chemistry of natural plasmas, such as the ionosphere and the interstellar medium, and of laboratory plasma media, such as gas laser systems, etchant plasmas and combustion plasmas. A great deal of relevant data has been obtained principally by exploiting the variable-temperature selected ion flow tube (VT-SIFT), the variable-temperature selected ion flow drift tube (VT-SIFDT) and the variable-temperature flowing afterglow/Langmuir probe (VT-FALP) techniques which were developed in our laboratory. Part of the overall programme is supported by a grant from the Science and Engineering Research Council.

Accession For	
NTIS GRA&I	☑
DTIC TAB	☐
Unannounced	☐
Justification	
By	
Distribution/	
Availability Codes	
Dist	Avail and/or Special
A-1	

DTIC
COPY
INSPECTED
1

I INTRODUCTION

Our major commitment under the terms of the current grant is to study various gas-phase ionic reaction processes at thermal and near-thermal energies, with special reference to processes that may occur in the terrestrial atmosphere and in combustion and discharge plasmas. Such processes include ion/neutral reactions, electron attachment, electron-ion recombination and ion-ion recombination (mutual neutralization). All these processes can be studied in our laboratory following our development and construction of the very versatile selected ion flow drift tube (SIFDT) and flowing afterglow/Langmuir probe (FALP) techniques. Using these techniques, rate coefficients and ion products of reactions can be determined in many cases over the wide temperature range 80-600K and at reactant ion/reactant neutral centre-of-mass energies up to about one electron volt in some cases. Numerous reactions have been studied during the past few years and many have been presented in previous reports and research publications. During the period covered by this interim report we have added laser and vacuum ultraviolet techniques to the already versatile FALP apparatus and this has greatly extended the processes that we can study. In this report we refer to the further studies we have made of electron attachment, electron-ion recombination, proton affinities of specific molecules and collisional breakup of molecular ions. Details of much of this work are given in the reprints and preprints of research papers which are included as appendices 1-5 of this report. A brief summary of the most important results are given in the next section.

II SUMMARY OF RESULTS

(a) Electron Attachment

We have determined the rate coefficients, β, for dissociative

1

attachment reactions of electrons with the unstable molecular radicals CCl_3 and CCl_2Br. These are the first measurements of the β for unstable radicals. The β are very large, being appreciable fractions of the maximum (capture) values, β_{max}, for such reactions, and this may have implications to the interpretation of data obtained from electron capture detectors. The results of this study are given in Appendix 1. It seems highly likely that dissociative attachment will occur for other halogenated molecular radicals.

Electron attachment studies of the halogenated benzenes C_6F_5Cl, C_6F_5Br and C_6F_5I have revealed that the β are quite large at 300K and increase towards the β_{max} with increasing temperature. Interestingly, different products result for each molecule; $C_6F_5Cl^-$ for C_6F_5Cl, predominantly $C_6F_5^-$ for C_6F_5I and predominantly $C_6F_5Br^-$ for C_6F_5Br at 300K but with Br^- becoming increasingly obvious as a product as the temperature increases, constituting ~40% of the product distribution at 450K. Comparison of these FALP data with previous data obtained in a time-of-flight experiment has enabled the autodetachment lifetime of nascent $C_6F_5I^-$ ions to be bracketted. Also from these FALP studies an upper limit to the C-Br bond dissociation energy in C_6F_5Br of 84 kcal mol^{-1} has been determined. The stability of the $C_6F_5^-$ ion was noted in these FALP studies and so a parallel SIFT study of the reactions of $C_6F_5^-$ ions with several molecular gases was carried out. This study and the attachment study are reported in detail in Appendix 2.

Other, as yet unpublished, studies of electron attachment to several halogenated ethanes have been carried out (i.e. CH_3CCl_3, $CH_2ClCHCl_2$, CF_3CCl_3, $CF_2ClCFCl_2$). The β for all these dissociative attachment reactions increase rapidly with increasing temperature and the product in every case is Cl^-. The β for the methyl and ethyl esters of triflic acid (i.e. $CF_3SO_3CH_3$ and $CF_3SO_3C_2H_5$) have also been measured and they

2

also increase rapidly with increasing temperature, but only reach the relatively small values of $4 \times 10^{-9} cm^3 s^{-1}$ and $9 \times 10^{-10} cm^3 s^{-1}$ respectively at ~500K, unlike triflic acid for which the β at 300K is close to β_{max}. The very stable $CF_3SO_3^-$ is the product ion in each of these reactions. The β for the reaction of $CFBr_3$ (producing Br^-), $C_6F_5CF_3$ (producing the parent negative ion) and $BrCN$ (CN^- is the exclusive product) have also been determined. The β for $BrCN$ is noteworthy in that it increases dramatically from $2.2 \times 10^{-9} cm^3 s^{-1}$ at 300K to 3.5×10^{-7} at 460K. These results will be properly appraised and reported in detail in a subsequent report.

(b) Electron-Ion Dissociative Recombination

The rate coefficients for dissociative recombination, α, for a wide variety of polyatomic ions, notably several protonated stable molecules, have been determined at 300K using the FALP apparatus. This is a simple procedure which exploits our discovery that H_3^+ ions do not recombine with electrons at a measurable rate when the ions are in their ground states ($\alpha \lesssim 10^{-10} cm^3 s^{-1}$ at 300K). So the addition of most stable molecular species, X, to an H_3^+ FALP plasma results in the production of XH^+ plasmas. By this means the α for many XH^+ can be determined. The α have been measured for species ranging in complexity from H_2F^+ to $(C_2H_5OH)_2H^+$ and these studies indicate that, in general, at 300K the α vary from about $10^{-7} cm^3 s^{-1}$ for the simple ions to ~$10^{-6} cm^3 s^{-1}$ for more polyatomic ions. The results of our most recent studies are given in Appendix 3 and a brief review of the status of FALP studies of dissociative recombination is given in Appendix 4.

The most exciting recent development is the addition of spectroscopic diagnostics to the FALP apparatus. Specifically, we have acquired a tunable dye laser system and a vacuum ultraviolet (VUV) monochromator to

add to the optical monochromator, the quadrupole mass spectrometer and the Langmuir probe diagnostics. With these spectroscopic techniques many more aspects of plasma reaction processes can be investigated. Our first major objective is to determine the neutral products of some dissociative recombination reactions, an unresearched field. To date in preliminary studies we have exploited laser induced fluorescence (LIF) to detect the presence, or otherwise, of OH radicals in recombining plasmas comprising ground state HCO^+, H_3O^+, CO_2H^+ and N_2OH^+ ions and electrons. As expected, no OH is generated when HCO^+ recombines with electrons but OH is a significant neutral product when the other three ions dissociatively recombine. Indeed, OH appears to be a major product of H_3O^+ recombination with electrons which implies that H_2O can only be a minor product (if it is a product at all). Before we can more accurately specify the neutral products of these reactions, we need to know if H atoms or O atoms are also formed. This we will investigate using VUV absorption at the resonance line frequencies for H atoms (121.6nm) and O atoms (130.2nm). These experiments have been commenced and the results of these pioneering studies will be given in the next report.

(c) Determinations of Proton Affinities

The proton affinity (PA) of atomic or molecular species is an important parameter since it determines whether or not a proton can transfer from a protonated species XH^+ to another species Y to form YH^+ and X. This is important to an understanding of the ion chemistry of real plasma media. Using the PA of C_2H_4 as a standard, we have determined accurately the PA of H_2O and CS_2 by determining the rate coefficients for proton transfer reactions using the SIFT apparatus. Thus the PA of H_2O has been determined to be 165.1 ± 0.7 kcal mol^{-1}. The detailed results of this study are given in Appendix 5. During the

4

course of this study we observed that $C_2H_5^+$ ions rapidly associated with H_2O to form ions with the molecular formula $C_2H_7O^+$ which could be protonated ethanol, $C_2H_5OH_2^+$. To investigate this, we have formed $C_2H_5OH_2^+$ from C_2H_5OH in an ion source, injected these ions into the SIFDT apparatus and observed that the ions formed in the ensuing collisional breakup of $C_2H_5OH_2^+$ are H_3O^+ and $C_2H_5^+$. We use this observation as evidence in support of the premise that the $C_2H_7O^+$ formed in the association of H_3O^+ with C_2H_4 is protonated ethanol. This work will be discussed in detail in a subsequent report.

III CONCLUSIONS

Significant progress has been made during the last year especially in the studies of electron attachment and dissociative recombination. Particularly significant is the addition of the LIF and VUV spectroscopic techniques to the FALP with all the potential they bring for the study of the neutral products of reactions, notably dissociative recombination reactions. Already, we have shown that OH is a major product of the dissociative recombination of ground state H_3O^+ ions. In other preliminary studies using the tunable laser we have investigated the photodetachment of electrons from some ground state negative ions (e.g. I^-, Cl^-, $CF_3SO_3^-$). The variety of processes that can be investigated using our SIFDT and FALP apparatuses is wide and we intend to pursue with vigour and imagination the several research objectives outlined in the grant application.

APPENDIX I

STUDIES OF DISSOCIATIVE ELECTRON ATTACHMENT TO THE FREE RADICALS

CCl_3 AND CCl_2Br USING THE FALP APPARATUS

N.G. ADAMS, D. SMITH and C.R. HERD

STUDIES OF DISSOCIATIVE ELECTRON ATTACHMENT
TO THE FREE RADICALS CCl_3 AND CCl_2Br
USING THE FALP APPARATUS

N.G. ADAMS, D. SMITH and C.R. HERD

*Department of Space Research, University of Birmingham, P.O. Box 363,
Birmingham B15 2TT (Gt. Britain)*

(Received 30 October 1987)

ABSTRACT

Measurements are reported of the rate coefficients, β, for the (secondary) dissociative attachment reactions of electrons with the unstable molecular radical species CCl_3 and CCl_2Br formed in the primary dissociative attachment reactions of electrons with CCl_4 and CCl_3Br molecules. This was achieved using the flowing afterglow/Langmuir probe (FALP) apparatus. The values of β for both the primary (β_1) and the secondary (β_2) attachment reactions are large, indicating that each CCl_4 and CCl_3Br molecule introduced into a sufficiently dense thermalized plasma will result in the rapid loss of two free electrons to form two negative halide ions. To our knowledge, these are the first measurements of β for unstable molecular radical species.

INTRODUCTION

Electron attachment has been studied over the last two decades using a variety of techniques. The texts by Christophorou [1] and Massey [2] describe much of the earlier work. Subsequently, new techniques have been developed to determine attachment rate coefficients, β, for many other reactions [3].

Our flowing afterglow/Langmuir probe (FALP) technique has recently been developed to determine β for attachment reactions under truly thermal conditions over the approximate temperature range from 200 to 600 K [4,5]. Thus, several dissociative and non-dissociative attachment reactions have been studied and the rate coefficients as well as energies of activation for several reactions have been determined over the above temperature range [6,7].

Electron attachment to CCl_4, which is very rapid, has been studied extensively by many investigators. In a previous paper [6], we summarized

the previous work, reported the value of β_1 determined in the FALP apparatus ($\beta_1 = 4.0 \times 10^{-7}$ cm^3 s^{-1}), and speculated that rapid secondary electron attachment to the unstable radical CCl$_3$ (produced via dissociative electron attachment of CCl$_4$) could be occurring in the afterglow plasma of the FALP apparatus. However, at that time, the occurrence of secondary attachment could not be positively demonstrated because the range of n_e measurable with the Langmuir probe was limited to n_e greater than about 10^9 cm^{-3}. The significance of this will be appreciated after a reading of the data analysis section of this paper. Subsequent to these earlier measurements, the Langmuir probe technique was improved and now values of n_e as small as 10^7 cm^{-3} can be measured. Hence, in this paper, we are now able to present conclusive evidence to support our previous speculation that CCl$_3$ undergoes a rapid dissociative attachment with thermal electrons. We also report that secondary dissociative attachment occurs between electrons and the unstable CCl$_2$Br radicals produced from the primary dissociative attachment reactions of electrons with CCl$_3$Br. Values of β_2 for these secondary attachment processes have been obtained, which, to our knowledge, are the first measurements of the electron attachment coefficients for unstable radical molecules.

EXPERIMENTAL

The FALP technique, which has been utilized for studies of ionic and electronic recombination as well as electron attachment, has been discussed in detail previously [5,6]. Basically, a thermalized helium afterglow plasma created by a microwave discharge is convected along the flow tube by a flowing helium carrier gas. Argon is added to the afterglow to destroy helium metastables (which could produce electrons down the length of the flow tube by Penning ionization) and attaching gases are then added to the thermalized afterglow. A mass spectrometer/detection system is located at the downstream end of the flow tube which is used to determine the positive and negative ion compositions of the flowing plasmas. A small, cylindrical Langmuir probe serves as the plasma diagnostic in determining the electron number density, n_e. The probe is movable along the flow tube (the z coordinate) and can be positioned at any point on the axis. Attachment rate coefficients are determined from the variation of the axial electron number density $n_e(z)$ with z.

All of the experiments were carried out at a helium pressure of ~ 1 torr and at 300 K. Because the molecules in this study react rapidly with electrons, the attaching gases were diluted with helium with accurately known mixing ratios of about 1%. The attaching gas number densities, n_r, at the injection port located 57.5 cm from the nose cone mass spectrometer

sampling orifice, were calculated from the flow rates of the attaching gases into the afterglow plasma.

DATA ANALYSIS

The determinations of $n_e(z)$ were carried out in the region of the flow tube where electron loss was due largely to attachment and, to a small extent only, to ambipolar diffusion (which was minimized by running at sufficiently higher helium pressure). The appropriate continuity equation describing this loss is

$$v_p \frac{\partial n_e(z)}{\partial z} = D_E \nabla^2 n_e(z) - \beta n_e(z) n_r \tag{1}$$

where v_p is the plasma velocity and D_e is the coefficient for ambipolar diffusion of electrons with the ambient positive ions. Because D_e is a function of n_-/n_e (where n_- is the negative ion number density), this equation cannot be solved analytically. However, Oskam [8] and Biondi [9] have derived an equation describing $n_e(z)$, which is

$$n_e(z) = \frac{n_e(0)}{1-(\nu_0/\nu_a)} \left[\exp\left(\frac{-\nu_a}{v_p} z \right) - \frac{\nu_D}{\nu_a} \exp\left(\frac{\nu_D}{v_p} z \right) \right] \tag{2}$$

where $\nu_D = D_e/\Lambda^2$, $\nu_a = n_r\beta$, and Λ is the characteristic diffusion length of the flow tube. In the derivation of Eq. (2), the quasi-neutrality condition
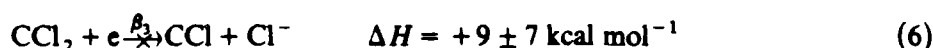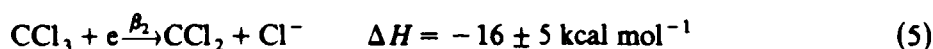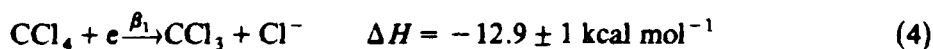
$$n_+(z) = n_-(z) + n_e(z)$$

was used and two basic assumptions were also made: (i) loss of positive ions is by diffusion only and (ii) the negative ions have no loss processes (neither reactive nor diffusive). The continuity equations for $n_+(z)$ and $n_-(z)$ can then be solved analytically to yield eq. (2). Using this equation, a curve-fitting routine can then be used to determine β_1. For measuring primary electron attachment rate coefficients in this way, n_e must be kept small (i.e. $n_e < n_r$), so that $n_r(z)$ remains constant. This allows n_e versus z data to be analyzed utilizing pseudo-first-order reaction kinetics. For values of n_e approaching and exceeding the initial reactant concentration, the electrons begin to remove the primary attaching gas from the afterglow and then pseudo-first order kinetics no longer apply. Equation (2) is then no longer valid since n_r is no longer constant in the reaction region of the FALP apparatus. Also, if the neutral radical molecules formed in the primary dissociative electron-attachment reaction (e.g. the CCl_3 resulting from the $CCl_4 + e$ reaction) dissociatively attach electrons (secondary attachment), then $n_e(z)$ will contain information on that process. In order to take into account this second-order kinetic behaviour, to obtain an expression for

$n_e(z)$ and thus to obtain values for the secondary attachment rate coefficients, β_2, it is necessary to rewrite the quasi-neutrality condition mentioned above as

$$\frac{\partial n_e(z)}{\partial z} = \frac{\partial n_+(z)}{\partial z} - \frac{\partial n_-(z)}{\partial z} \tag{3}$$

The rate of change of $n_+(z)$ with z, i.e. the z gradient of n_+ ($\partial n_+(z)/\partial z$), is again assumed to result from ambipolar diffusion only, whilst the z gradient of n_- (i.e. $\partial n_-(z)/\partial z$), is now modelled assuming second-order kinetic behaviour which is represented by the linear first-order differential equation representing its production mechanisms for the particular attachment processes under consideration. (It is again assumed that there are no loss processes for negative ions.) Thus, for example, for electron attachment to CCl_4 for which both primary and secondary attachment can occur (but not tertiary attachment)

$$CCl_4 + e \xrightarrow{\beta_1} CCl_3 + Cl^- \qquad \Delta H = -12.9 \pm 1 \text{ kcal mol}^{-1} \tag{4}$$

$$CCl_3 + e \xrightarrow{\beta_2} CCl_2 + Cl^- \qquad \Delta H = -16 \pm 5 \text{ kcal mol}^{-1} \tag{5}$$

$$CCl_2 + e \xrightarrow{\beta_3} CCl + Cl^- \qquad \Delta H = +9 \pm 7 \text{ kcal mol}^{-1} \tag{6}$$

[where the exothermicities of reactions (4) and (5) and the endothermicity of reaction (6) are calculated from the thermochemical data obtained from refs. 10 and 11], the appropriate differential equations describing CCl_4 loss, CCl_3 formation and loss, and Cl^- formation are

$$v_p \frac{\partial [CCl_4]}{\partial z} = -\beta_1 [CCl_4] n_e \tag{7}$$

$$v_p \frac{\partial [CCl_3]}{\partial z} = -(\beta_2 [CCl_3] n_e - \beta_1 [CCl_4] n_e) \tag{8}$$

$$v_p \frac{\partial [Cl^-]}{\partial z} = \beta_1 [CCl_4] n_e + \beta_2 [CCl_3] n_e \tag{9}$$

where the square brackets denote concentrations. Because Eqs. (7)-(9) are coupled, it is necessary to solve them numerically. Two numerical methods were employed, the Euler method and the classical fourth-order Runge-Kutta method [12]. These methods involved incrementing z by a small element, Δz, and calculating (using a microcomputer) the increments in and thus the magnitudes of $[CCl_4]$, $[CCl_3]$ and $[Cl^-]$ [or, equivalently, $n_-(z)$] at position $z + \Delta z$ utilizing Eqs. (7)-(9). The value of $n_+(z + \Delta z)$ was determined using the differential equation

$$v_p \frac{\partial n_+(z)}{\partial z} = -\frac{D_e}{\Lambda^2} n_+(z) \tag{10}$$

10

which, for convenience, was also solved by the numerical methods mentioned above. Then, rewriting the quasi-neutrality condition as

$$n_e(z + \Delta z) = n_+(z + \Delta z) - n_-(z + \Delta z) \tag{11}$$
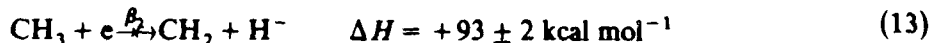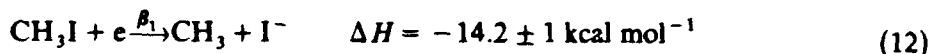
enabled $n_e(z + \Delta z)$ to be determined. By this procedure, plots of $\log n_e$ versus z were constructed for various initial conditions [various values of $n_e(0)$, and thus $n_+(0)$, $n_r(0)$, β_1, and β_2] and compared with experimental $n_e(z)$ data. The terms $n_e(0)$ and $n_r(0)$ represent the initial values of $n_e(z)$ and $n_r(z)$ used in the numerical analysis. A step size, Δz, of 0.1 cm was found to be sufficiently small; any further decrease in Δz below this value did not noticeably influence the fit. It was observed that the simpler Euler method gave essentially the same fit as the inherently more accurate Runge–Kutta method, which was consistently used to analyze the data.

So, the procedure used in the present studies was first to determine $n_e(z)$ experimentally as a function of z for $n_e(0) < n_r(0)$ and then apply the above analysis procedure to obtain a value of β_1, i.e. the β for the primary reaction step. Next, $n_e(z)$ was determined as a function of z when $n_e(0) > n_r(0)$ to permit the determination of β_2, i.e. β for the secondary step(s) (if they occur). Such experiments were performed for both CCl_4 and CCl_3Br. Firstly, however, as a test of our analytical method, dissociative electron attachment to CH_3I (giving CH_3 and I^-) was studied since this is a simpler situation in which secondary electron attachment to CH_3 does not occur at thermal energies.

RESULTS

The attachment reaction of CH_3I

This study was carried out for four initial values of $n_e(0)$ to illustrate the method of analysis and to demonstrate the phenomenon of neutral reactant depletion while avoiding the complication of secondary electron attachment. The reaction is

$$CH_3I + e \xrightarrow{\beta_1} CH_3 + I^- \qquad \Delta H = -14.2 \pm 1 \text{ kcal mol}^{-1} \tag{12}$$

$$CH_3 + e \xrightarrow{\beta_2} CH_2 + H^- \qquad \Delta H = +93 \pm 2 \text{ kcal mol}^{-1} \tag{13}$$

The results of the study are shown in Fig. 1. The symbols represent the experimental data points while the continuous curves are values of $n_e(z)$ calculated utilizing the curve-fitting routine. Curve A describes the situation for which $n_e(0) < n_r(0)$ and therefore for conditions such that significant depletion of $n_r(z)$ (due to attachment) in the reaction region of the flow tube does not occur. The fit shown is obtained with a value of $\beta_1(CH_3I)$ of 1.2×10^{-7} cm^3 s^{-1}, which is in agreement with our previously published value at 300 K. [7]
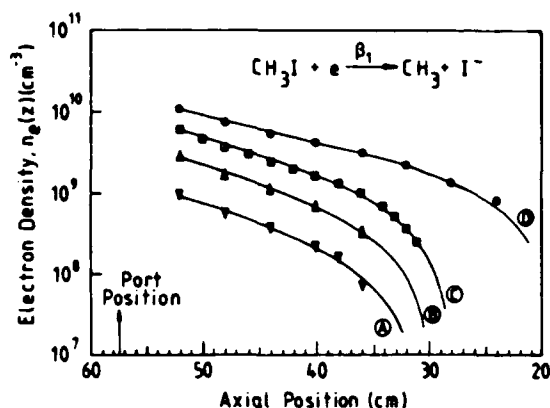
Fig. 1. Plots of electron density, $n_e(z)$, determined as a function of axial position, z, in the FALP for the dissociative attachment reaction of electrons with CH_3I. The four sets of experimental data (symbols) were obtained at an initial attaching gas number density, n_r, of 7.5×10^9 cm^{-3}. For the higher initial electron densities, i.e. the ■ and ● data, $n_r(z)$ is depleted by the attachment process whereas no significant depletion occurs for the lower initial electron densities, i.e. the ▼ and ▲ data. All data were obtained at a helium pressure of ~1 torr and at 300 K. The solid curves A–D represent computer fits (see text) using a primary attachment coefficient, $\beta_1(CH_3I)$, of 1.2×10^{-7} cm^3 s^{-1} and taking into account the depletion of the attaching gas.

Curves B–D in Fig. 1 represent the situations for which n_e was increased towards and beyond $n_r(0)$ and thus conditions for which reactant depletion occurs to an increasing extent. A fixed value of $\beta_1(CH_3I) = 1.2 \times 10^{-7}$ cm^3 s^{-1} is used under these circumstances. Note that the fits of the generated curves to the experimental data (accounting for reactant depletion and with $\beta_2 = 0$) are excellent. For curves C and D, $n_e(0) > n_r(0)$, in which cases $n_r(z)$ was reducing along the length of the flow tube [i.e a variation in $n_r(z)$ resulted]. For these conditions, $n_r(z)$ had actually reduced somewhat between the entry port and the position downstream where complete mixing of the attaching gas with the helium occurred (typically 2–4 cm from the port), which is the position where the determination of $n_e(z)$ began. The net effect of this is that $n_r(0)$ is somewhat less than n_r with this reduction being greater the greater the initial value of n_e. Thus, to obtain the fits for curves C and D in Fig. 1, $n_r(0)$ values some 2 and 18% less than n_r, respectively, were used. For curves A and B (i.e. low values of n_e), values of $n_r(0)$ equal to n_r were used.

The attachment reaction of CCl$_4$

Figure 2(a) shows experimental data points (symbols) for four initial values of $n_e(0)$. The continuous curves indicate the predicted $n_e(z)$ account-
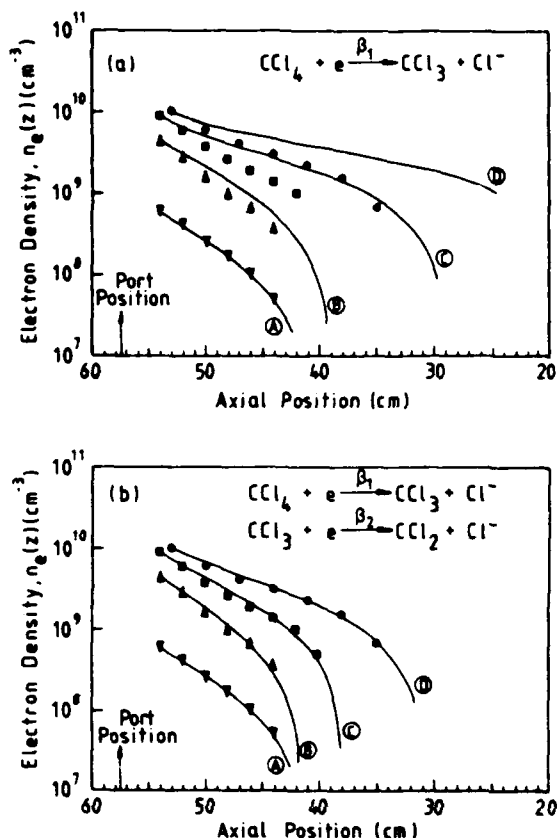
Fig. 2. Plots of electron density, $n_e(z)$, as a function of axial position, z, in the FALP for the dissociative attachment reaction of electrons with CCl_4. The four sets of experimental data (symbols) represented in both (a) and (b) were obtained at an initial CCl_4 number density, n_r, of $5.0 \times 10^9 \, cm^{-3}$. For the higher initial electron densities, i.e. the ■ and ● data, $n_r(z)$ is depleted by the attachment process whereas no significant depletion occurs for the lower initial electron densities, i.e. the ▼ and ▲ data. All data were obtained at a helium pressure of ~1 torr and at 300 K (for details see text).

ing for reduction of the CCl_4 concentration [i.e $n_r(z)$] but not accounting for the secondary attachment reaction of the CCl_3 radicals generated in the primary reaction, i.e. setting the attachment coefficient for the reaction of CCl_3 radicals, $\beta_2(CCl_3)$, equal to 0. The discrepancy between the experimental points and the fitted curves B–D [for which $n_e(0) > n_r(0)$] is obvious and this is a clear indication of a secondary electron attachment reaction between the CCl_3 radicals and electrons (compare with the data in Fig. 1 in which a secondary attachment reaction involving CH_3 does not occur). Curve A, in which the fit between experimental and calculated values of $n_e(z)$ is excellent, is for conditions such that $n_e(0) < n_r(0)$ and for a
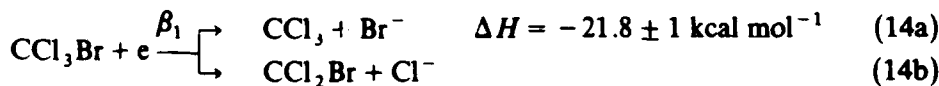
$\beta_1(CCl_4) = 4.2 \times 10^{-7}$ cm^3 s^{-1}. This value is, within error, in good agreement with our previously reported value of 4.0×10^{-7} cm^3 s^{-1} [3] [see ref. 3 for a compilation of other reported values for $\beta_1(CCl_4)$].

In Fig. 2(b), plots of the same experimental points as in Fig. 2(a) are shown and are now compared with generated curves which account for a finite $\beta_2(CCl_3)$. We determined that a value of $\beta_2(CCl_3) = 2.4 \times 10^{-7}$ cm^3 s^{-1} gives the best overall fit to the three data sets B–D and these fits are shown in Fig. 2(b). As stated above, tertiary attachment to CCl_2 cannot occur at a significant rate since this process is endothermic [see reaction (6)]. Thus, for this system, each CCl_4 molecule removes two electrons from a thermal plasma in which there are sufficient electrons. Again, for curves A and B, $n_r(0)$ was taken as equal to n_r while, for curves C and D, $n_r(0)$ was 13 and 19%, respectively, less than n_r to obtain the fits shown in Fig. 2(b).
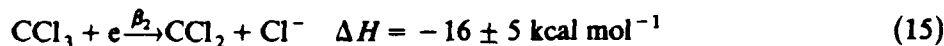
This is, to our knowledge, the first measurement of the β for dissociative attachment reactions of electrons with unstable radicals. The net result for electron attachment to CCl_4 at thermal energies is as follows: $\beta_1(CCl_4)$, the primary attachment rate coefficient, is $(4.2 \pm 0.6) \times 10^{-7}$ cm^3 s^{-1} while for the secondary step of electron attachment to CCl_3, $\beta_2(CCl_3) = (2.4 \pm 1) \times 10^{-7}$ cm^3 s^{-1}. The error figures are those resulting from the fitting routine as well as from the systematic errors inherent in the experiment.

The attachment reaction of CCl_3Br

For the reactions

$$CCl_3Br + e \xrightarrow{\beta_1} \begin{cases} CCl_3 + Br^- & \Delta H = -21.8 \pm 1 \text{ kcal mol}^{-1} \quad (14a) \\ CCl_2Br + Cl^- & \quad (14b) \end{cases}$$

$$CCl_3 + e \xrightarrow{\beta_2} CCl_2 + Cl^- \quad \Delta H = -16 \pm 5 \text{ kcal mol}^{-1} \quad (15)$$

$$CCl_2Br + e \xrightarrow{\beta_2} \begin{cases} CCl_2 + Br^- & \quad (16a) \\ CClBr + Cl^- & \quad (16b) \end{cases}$$

the experimental data (symbols) are shown in Fig. 3(a) and (b). Again, $\beta_1(CCl_3Br)$ was obtained from curve A for which $n_e(0) < n_r(0)$. Thus, the total rate coefficient for the primary reaction of electrons with CCl_3Br, i.e. $\beta_1(CCl_3Br)$, in which both Cl^- and Br^- are produced was determined to be 8.2×10^{-8} cm^3 s^{-1}. The branching ratio for Cl^- and Br^- production in the reaction is $Cl^- \sim 55\%$ and $Br^- \sim 45\%$ as determined using the quadrupole mass filter under conditions such that $n_e(0) < n_r(0)$.

The continuous curves in Fig. 3(a) represent values of $n_e(z)$ calculated with $\beta_1(CCl_3Br) = 8.2 \times 10^{-8}$ cm^3 s^{-1}, $\beta_2(CCl_3) = 2.4 \times 10^{-7}$ cm^3 s^{-1} (determined from the CCl_4 experiments), and $\beta_2(CCl_2Br) = 0$. The poor fit
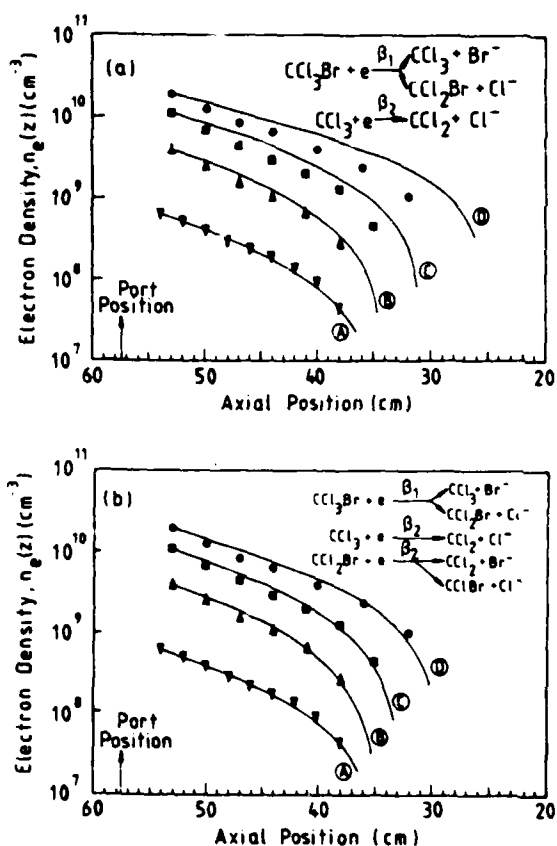
Fig. 3. Plots of electron density, $n_e(z)$, determined as a function of axial position, z, in the FALP for the primary dissociative attachment reaction of electrons with CCl_3Br producing both Cl^- (together with CCl_2Br radicals) and Br^- (with CCl_3 radicals) and for the secondary attachment of electrons with the product radicals. The four sets of experimental data (symbols) represented in (a) and (b) were obtained at an initial CCl_3Br number density, n_r, of 1.1×10^{10} cm^{-3}. For the higher initial electron densities, i.e. the ■ and ● data, the CCl_3Br number density is depleted by the attachment process whereas no significant depletion occurs for the lower initial electron densities, i.e. the ▼ and ▲ data. All data were obtained at a helium pressure of ~1 torr and at 300 K (for details see text).

between the experimental points and the calculated curves for $n_e(0) > n_r(0)$ is clear evidence that electron attachment to the unstable radical CCl_2Br is occurring. The value of $\beta_2(CCl_2Br)$ is determined by adjusting its magnitude in the calculation to give the best fit to the experimental data. Figure 3(b) shows the fit that is obtained with $\beta_2(CCl_2Br) = 1.5 \times 10^{-7}$ cm^3 s^{-1}. The fitted curves A and B in Fig. 3(b) were obtained with $n_r(0)$ equal to n_r whereas, for curves C and D, $n_r(0)$ values 13 and 19%, respectively, less than n_r were used.

In summary, the results for CCl_3Br attachment reveal that $\beta_1(CCl_3Br) = (8.2 \pm 1.2) \times 10^{-8}$ cm^3 s^{-1}, $\beta_2(CCl_3) = (2.4 \pm 1) \times 10^{-7}$ cm^3 s^{-1}, and $\beta_2(CCl_2Br)$ is of the order of $1 \times 10^{-7} cm^3 s^{-1}$. Also, as $n_e(0)$ was increased, the percentage of Cl^- increased from $\sim 55\%$ at the lowest $n_e(0)$ to $\sim 65\%$ at the highest $n_e(0)$. This may indicate that Cl^- production via reaction (15) and/or (16b) is favoured relative to reaction (16a). This, of course, would give three possible pathways for Cl^- production.

CONCLUSION

The principles of the method we have applied to the determination of attachment coefficients, β, using the FALP are straightforward. When the electron number density, n_e, in the thermalized plasma is adjusted to be much smaller than the attaching molecule number density, n_r, then there is a straightforward analytical procedure for determining the β value for the primary attachment reaction from the variation of n_e with z, i.e. $n_e(z)$. Under these circumstances, pseudo-first-order kinetics for n_e loss are applicable, as we have shown in previous measurements of β for several species. When n_e is increased towards and beyond n_r, then depletion of the attaching gas occurs along the afterglow plasma. Under these different circumstances, $n_e(z)$ contains information about the variation of n_r with z, i.e. $n_r(z)$, and this shows whether or not secondary attachment reactions are occurring which involve the neutral radical products of the primary attachment reaction. Analysis of the data for the molecules CCl_4 and CCl_3Br, which undergo rapid dissociative attachment reactions with electrons, has shown that the product radicals CCl_3 and CCl_2Br do indeed undergo dissociative attachment reactions with electrons. Thus, these gases, especially CCl_4, are very efficient in removing electrons from thermal plasmas. The tertiary attachment reaction of CCl_2 radicals does not occur at thermal energies since this process is endothermic. Other halogenated hydrocarbons presumably produce radicals (via primary dissociative attachment reactions) that also undergo dissociative attachment reactions with electrons. The phenomenon of secondary attachment has implications in the use of electron-capture detectors for the quantitative determination of halogenated hydrocarbon concentrations since, in some cases, each molecule will remove more than one electron. Further work is proceeding to investigate this phenomenon.

REFERENCES

1 L.G. Christophorou, Atomic and Molecular Radiation Physics, Wiley-Interscience, New York, 1971.
2 H.S.W. Massey, Negative Ions, Cambridge University Press, Cambridge, 1976.
3 L.G. Christophorou, D.R. James and R.Y. Pai, in H.S.W. Massey, E.W. McDaniel and B. Bederson (Eds.), Applied Atomic Collision Physics, Vol. 5, Academic Press, New York, 1982.
4 D. Smith and M.J. Church, Int. J. Mass Spectrom. Ion Phys., 19 (1976) 185.
5 E. Alge, N.G. Adams and D. Smith, J. Phys. B, 16 (1983) 1433.
6 D. Smith, N.G. Adams and E. Alge, J. Phys. B, 17 (1984) 461.
7 E. Alge, N.G. Adams and D. Smith, J. Phys. B, 17 (1984) 3827.
8 H.J. Oskam, Philips Res. Rep., 13 (1958) 335.
9 M.A. Biondi, Phys. Rev., 109 (1958) 2005.
10 T.M. Miller, in R.C. Weast (Ed.), CRC Handbook of Chemistry and Physics, CRC Press, Boca Raton, FL, 66th edn., 1985, p. E-67. J.A. Kerr, in R.C. Weast (Ed.), CRC Handbook of Chemistry and Physics, CRC Press, Boca Raton, FL, 66th edn., 1985, pp. F-174–F-194.
11 JANAF Thermochemical Tables, National Bureau of Standards, Washington, DC, 2nd edn., 1971.
12 C.F. Gerald, Applied Numerical Analysis, Addison-Wesley, Reading, MA, 1980.

APPENDIX 2

FALP STUDIES OF ELECTRON ATTACHMENT REACTIONS OF

C_6F_5Cl, C_6F_5Br AND C_6F_5I

C.R. HERD, N.G. ADAMS and D. SMITH

FALP STUDIES OF ELECTRON ATTACHMENT REACTIONS OF

C_6F_5Cl, C_6F_5Br AND C_6F_5I

CHARLES R. HERD, NIGEL G. ADAMS AND DAVID SMITH

Department of Space Research

University of Birmingham

Birmingham B15 2TT (Gt. Britain)

ABSTRACT

Electron attachment reactions of thermal electrons with C_6F_5Cl, C_6F_5Br and C_6F_5I molecules have been studied at 300 and 450K using the flowing afterglow/Langmuir probe (FALP) technique. The rate coefficients at both temperatures are large and increase with increasing temperature. Different ionic products are obtained in the reactions; $C_6F_5Cl^-$ only for C_6F_5Cl, predominantly $C_6F_5^-$ for C_6F_5I, and predominantly $C_6F_5Br^-$ at 300 K for C_6F_5Br with the percentage of Br^- increasing with increasing temperature and constituting ~40% of the total products at 450 K. Comparison of these "high pressure" FALP data with previous "low pressure" data obtained from an ion beam time-of- flight experiment, has enabled the autodetachment lifetime of the excited intermediate ion $(C_6F_5I^-)^*$ to be bracketed between 10^{-7} and 10^{-6}s. Also an upper limit to the C-Br bond dissociation energy in C_6F_5Br of ~ 84 kcal mol^{-1} has been determined from a consideration of the kinetics of the C_6F_5Br reaction. In a parallel study, the reactions of $C_6F_5^-$ ions with several molecular gases have been studied using a SIFT apparatus and these results are reported in an appendix.

INTRODUCTION

Electron attachment reactions have been studied using a variety of techniques which fall into two distinct categories, (i) low pressure techniques in which electrons interact with molecules, M, forming an excited negative ion $(M^-)^*$ which does not suffer collisions with ambient molecules during its lifetime, and (ii) high pressure techniques in which collisions of $(M^-)^*$ can occur which can modify the internal energy of $(M^-)^*$. The first category includes ion beam (time-of-flight, t.o.f.)[1] ICR [2] and photoionization cell [3] techniques, and the second category includes drift tube [4], Cavalleri [5] and FALP [6, 7] techniques. Attachment reactions are classified according to the observed products; when the negative ion products are the parent molecular negative ions (e.g. SF_6^- from SF_6 and $C_7F_{14}^-$ from C_7F_{14}) then the process is termed non-dissociative attachment, but when the product ions are fragments of the molecules (e.g. Cl^- from CCl_4, Br^- from CH_3Br) then the process is called dissociative attachment. In some electron/molecule reactions both dissociative and non-dissociative product channels are evident (e.g., SF_5^- and SF_6^- from SF_6 at temperatures $\geq$ 400K, and Br^- and $C_6F_5Br^-$ from C_6F_5Br, see below).

The capture of an electron by a molecule may result in the rapid and spontaneous dissociation to the fragment negative ion and a neutral atom or molecule (e.g. $CCl_4 + e \longrightarrow Cl^- + CCl_3$). The rate coefficient (or cross section) for the process then depends on the efficiency of the electron capture step which is usually dependent on the interaction temperature and energy of the reactants but not on the pressure of the ambient gas, since the dissociative attachment will usually occur on a timescale much shorter than the collision time, r_c, of $(M^-)^*$ with an

ambient atom or molecule (except at very large ambient gas pressures). However, when $(M^-)^*$ has an appreciable lifetime against autodetachment, τ_a, such that $\tau_a > \tau_c$, then superelastic collisions with ambient molecules can reduce the internal energy of $(M^-)^*$ and prevent autodetachment thus leading to the stable parent negative ion, M^-, or modify the product ion distribution (i.e. as between parent ions or fragment ions, see below). For such reactions it is to be expected that differences will be evident between the rate coefficients and product ion distributions determined using low pressure and high pressure methods and this is a major point to be drawn by comparing the results of the collision-dominated FALP experiments reported in this paper with those obtained from earlier low pressure experiments. It is worthy of note here that when τ_a is long (but necessarily $\ll \tau_c$) then the excited ion $(M^-)^*$ may be stabilized by the emission of an infrared photon. Several such $(M^-)^*$ have been identified in ICR experiments [2] and the radiative lifetimes, τ_r, have been determined.

During the last few years, we have developed the flowing afterglow/Langmuir probe (FALP) technique to study electron attachment reactions and to determine attachment rate coefficients, β, and product ion ratios [6, 7]. Thus the β have been determined for a number of dissociative and non-dissociative attachment reactions over a temperature range of about 200-600K in helium carrier gas at a pressure of about one torr. In all of the reactions studied, except that of hexafluorobenzene, C_6F_6, the β for each reaction was either sensibly independent of temperature over the available range, or increased with temperature and then "activation energies" were determined for the reactions. The β for the reaction of electrons with C_6F_6 (in which only the parent ion $C_6F_6^-$ was formed) very surprisingly was observed to decrease dramatically

with increasing temperature [8]. This anomalous behaviour was subsequently verified using different techniques [9, 10]. However, no totally convincing explanation for this behaviour has yet been given [11]. In pursuit of a better understanding of this unusual phenomenon, we chose to study electron attachment to the monosubstituted perfluorobenzenes C_6F_5Cl, C_6F_5Br, and C_6F_5I using the FALP apparatus.

Naff et al [1] studied these reactions some years ago using their elegant and productive t.o.f. mass spectrometer method. For these C_6F_5X molecules (X = Cl, Br, I), and for ill-defined electron energies <0.1 eV in their ion source, they observed that X^- and $C_6F_5^-$ ions were formed in all three cases. The ratios of the maximum current levels of X^- to $C_6F_5^-$ were 100 : 1, 3 : 1 and 1 : 3 for X = Cl, Br and I respectively. The parent ions $C_6F_5Cl^-$ and $C_6F_5Br^-$ were also observed and the autodetachment lifetimes, τ_a, were determined to be 17.6μs and 20μs respectively for the excited ions $(C_6F_5Cl^-)^*$ and $(C_6F_5Br^-)^*$. $C_6F_5I^-$ was not observed, indicating that τ_a for any $(C_6F_5I^-)^*$ formed was <1μs which was the smallest τ_a measurable in the t.o.f. experiment. Conditions in the FALP plasma are, of course, quite different than in the t.o.f. experiment. In the FALP plasma the ion collision times with carrier gas (helium) atoms, τ_c, is about 10^{-7}s which is much smaller than the τ_a given above for the $(C_6F_5Cl^-)^*$ and $(C_6F_5Br^-)^*$ ions. Also, since the temperatures of the reactant electrons and molecules - and hence their interaction energies - are precisely defined in the FALP, then differences in the product ion distributions of X^-, $C_6F_5^-$ and $C_6F_5X^-$ between the FALP and t.o.f. experiments are to be expected.

EXPERIMENTAL

The FALP technique has been described in detail previously [6, 7] and its application to the study of electron attachment has been thoroughly described in other papers [6, 7, 12]. Briefly, a thermalised afterglow plasma is created in helium carrier gas at about 1 torr pressure flowing along a flow tube (which is about 100 cm long and 8 cm in diameter) with a mass spectrometer sampling system located at the downstream end to identify the positive ion and/or negative ion types which, with free electrons, comprise the plasma. Controlled amounts of electron attaching gases are introduced into the thermalised flowing plasma and the modification of the gradient in the electron number density, n_e, along the axis of the flow tube (z-direction) due to the attachment process is determined using a Langmuir probe that can be positioned anywhere along the axis of the flow tube. Attachment coefficients, β, are derived from the analysis of the n_e versus z data obtained at fixed flow rates of the attaching gas into the afterglow [12]. The attachment reactions which are the subject of this paper are very rapid at the two temperatures for which measurements were made (300K and 450K, see Table 1) and so only very small number densities ($\sim 10^{10} cm^{-3}$) of the attaching gases were required to establish workable gradients of n_e along z. Thus, dilute (about 1%), accurately known mixes of the C_6F_5X gases with helium were made up to facilitate he accurate determination of the flow rates of C_6F_5X into the afterglow plasma. Since the number densities of the attaching molecules are so small, ion-molecule reactions cannot occur to any significant extent along the axis of the flow tube and so the product ions of the attachment reactions, as determined by the downstream mass spectrometer, are not confused. The values of β determined in this study are considered to be accurate to

±25%, although relative values of β for the different reactions are more accurate.
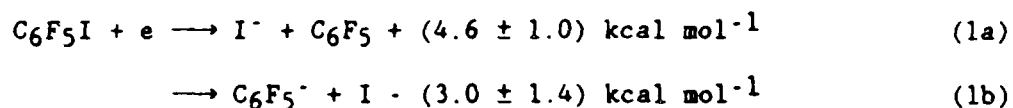
RESULTS AND DISCUSSION

As was previously mentioned, earlier FALP studies showed that β for the attachment of electrons to C_6F_6 decreased dramatically with increasing temperature and that only the parent ion $C_6F_6^-$ was observed as a product of the reaction. Naff et al [1] have measured the τ_a for $(C_6F_6^-)^*$ to be 12μs. Longer autodetachment lifetimes of >30μs [13] and ~50μs [14] have been measured for $(C_6F_6^-)^*$ formed by electron transfer to C_6F_6 from Rydberg atoms. It is apparent that these τ_a are much greater than the τ_c in the FALP plasma so all the $(C_6F_6^-)^*$ formed in the FALP plasma could be collisionally stabilized. Since there are no exothermic dissociative channels in the C_6F_6 attachment reaction then the observation that $C_6F_6^-$ is the only product ion is understandable. This same argument applies to the C_6F_5Cl reaction and therefore only the parent negative ion was observed to be formed in the FALP plasma. However, for both the C_6F_5Br and C_6F_5I reactions, dissociative channels are observed in the FALP experiments; notable is the attachment reaction of C_6F_5I in which the major product ion was $C_6F_5^-$. (In a parallel project, we have studied various ion-molecule reactions of $C_6F_5^-$ using a selected ion flow tube (SIFT) apparatus and the results are presented in the Appendix.)

As expected, some differences are apparent between the FALP data and the t.o.f. data of Naff et al [1]. Consideration of the FALP and t.o.f. data provides information concerning the thermochemistry of these attachment reactions and the lifetimes of the excited $(C_6F_5X^-)^*$ ions.

25

The reactions of C_6F_5I, C_6F_5Cl and C_6F_5Br are discussed separately below in the order stated.

1.   *Electron Attachment to C_6F_5I*

For this attachment reaction the major product was $C_6F_5^-$ (>95%) at both 300 and 450K. The parent ion $C_6F_5I^-$ was a minor product at 300K and only a trace of I^- was observed at 450K (see Table 1). A consideration of the thermochemistry for the two dissociative product channels gives:

$$C_6F_5I + e \longrightarrow I^- + C_6F_5 + (4.6 \pm 1.0) \text{ kcal mol}^{-1} \qquad (1a)$$
$$\longrightarrow C_6F_5^- + I - (3.0 \pm 1.4) \text{ kcal mol}^{-1} \qquad (1b)$$

The reaction ergicities were calculated using the accurately known electron affinity of I atoms, $EA(I) = (70.482 \pm .023)$ kcal mol^{-1} [15], and the less certain values of $EA(C_6F_5) \approx (63.2 \pm 1.0)$ kcal mol^{-1} [16, 17] and the bond dissociation energy $D(C_6F_5-I) = (66.2 \pm 1.0)$ kcal mol^{-1} [18].

It is interesting that the major product ion is $C_6F_5^-$ since this product channel is apparently endothermic whereas the exothermic I^- product is minimal. Similar behaviour has been observed by Compton and Reinhardt [17] for the collisional ionization of C_6F_6 by fast alkali atoms i.e., the more endothermic production of $C_6F_5^-$ appeared at a lower centre- of- mass energy than that for the less endothermic production of F^-. The reason for this type of behaviour is not yet understood; however, consideration of the availability of acceptor states for the free electron favours electron attachment to the multi-state polyatomic C_6F_5 radical rather than the singlet ground state I^-. The derived
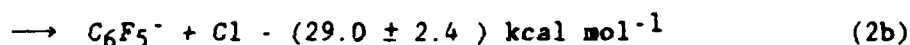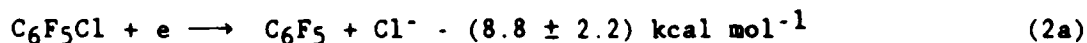
endothermicity of channel (1b) is not inconsistent with the present data
if the following argument can be accepted. The β values for the reaction
at both temperatures are appreciable fractions of the upper limit
(collisional) value, β_{max}, which we estimate to be about 2 - 3 x
$10^{-7} cm^3 s^{-1}$ (using the theory of Klots [19]). The β at 300K is measured
to be 3.2 x $10^{-8} cm^3 s^{-1}$ (see Table 1), and if this value is less than the
β_{max} by virtue of the reaction endothermicity or an activation energy
barrier, ΔE, then assuming a simple Boltzmann relationship (i.e. $\beta - \beta_{max}$
exp - $\Delta E/RT$) the ΔE is calculated to be about 1.2 kcal mol^{-1}. Also, if
the factor-of-four larger value of the measured β at 450K (see Table 1) is
also attributed to the effect of ΔE then combining the β values at the
two temperatures and again assuming the simple Boltzmann law, the ΔE is
calculated to be about 2.2 kcal mol^{-1}. It should be said that from these
measurements it is not possible to distinguish between an activation
energy barrier or an endothermicity. However it is notable that if the
ΔE is assumed to be due to an endothermicity then it is entirely
consistent with the ΔE calculated above for $C_6F_5^-$ production (reaction
(1b)). On this basis, the $D(C_6F_5-I)$ and the $EA(C_6F_5)$ adopted in the
calculation of ΔE are seemingly quite accurate (to within about 1 kcal
mol^{-1} as indicated above).

As mentioned above, the parent ion $C_6F_5I^-$ was discernible in the
product ion spectrum at 300K in the FALP experiment whereas in the t.o.f.
experiments of Naff et al [1], in which negative ions with lifetimes $\leq 1\mu s$
could not be detected, parent ions were not detected. Hence the
implication is that $(C_6F_5I^-)^*$ has a $\tau_a < 1\mu s$ but greater than the τ_c in
the FALP plasma which is about $0.1\mu s$. This therefore brackets the τ_a of
$(C_6F_5I^-)^*$ between $10^{-7}s$ and $10^{-6}s$. The lower limit to τ_a may be somewhat
greater than that quoted since helium, in general, inefficiently

collisionally stabilizes excited ions and so several collisions may be needed to stabilize the $(C_6F_5I^-)^*$. In view of this, it seems probable that the τ_a for $(C_6F_5I^-)^*$ at 300K is close to 10^{-6}s. Also, because $C_6F_5I^-$ is absent from the product ion spectrum at 450K a significantly lower τ_a for $(C_6F_5I^-)^*$ at this higher temperature is indicated.

2. Electron Attachment to C_6F_5Cl

The parent negative ion $C_6F_5Cl^-$ was the only significant product ion observed in the FALP experiment at both temperatures, whereas both $C_6F_5Cl^-$ and Cl^- were produced in the ion source of the t.o.f. experiment [1]. Cl^- and $C_6F_5^-$ production are both quite endothermic:

$$C_6F_5Cl + e \longrightarrow C_6F_5 + Cl^- - (8.8 \pm 2.2) \text{ kcal mol}^{-1} \qquad (2a)$$
$$\longrightarrow C_6F_5^- + Cl - (29.0 \pm 2.4) \text{ kcal mol}^{-1} \qquad (2b)$$

and thus the truly thermal FALP experiment is consistent with these energetics. The reaction ergicities were calculated using $EA(Cl)=$ $(83.336 \pm .092)$ kcal mol^{-1} [15], $D(C_6F_5\text{-}Cl) = (92.2 \pm 2.2)$ kcal mol^{-1}[20] and the $EA(C_6F_5)$ as given in sub-section 1. The long τ_a of 17.6μs for the $(C_6F_5Cl^-)^*$[1] together with the large β measured in the FALP experiment (which are appreciable fractions of β_{max} at both temperatures, see Table 1), implies that thermal electrons are efficiently captured by the C_6F_5Cl molecules and that the $(C_6F_5Cl^-)^*$ ions are effectively stabilized in collisions with He atoms. The increase in β with temperature (in this case about a factor of 2 between 300K and 450K) is not uncommon for non- dissociative attachment reactions and could be a manifestation of a small activation energy barrier to electron capture

(equated to ΔE) which as before, is estimated from the kinetics to be -1.3 kcal mol^{-1}. It is unlikely to be due to a variation of r_a with temperature (since $r_a \gg r_c$) or a variation of the collisional stabilization efficiency of $(C_6F_5Cl^-)^*$ by He atoms over such a relatively small temperature range. It is worthy of note that the sense of the β dependence on temperature is opposite to that for the β for non-dissociative attachment to C_6F_6 (the C_6F_6 case has been discussed in detail in previous papers [8-11]). A final note worth making here is that the observation of Cl$^-$ as a major product in the t.o.f. experiment implies that a fraction of the electrons in the t.o.f. ion source must be suprathermal by at least 0.3eV (rather than the upper limit energy of 0.1 eV indicated by Naff et al [1]) if the energetics given with the equation (2a) are correct . Alternatively, the literature value for $D(C_6F_5-Cl)$ may be too large by a few kcal mol^{-1} .

3. Electron Attachment to C_6F_5Br

The major product ions of this reaction were $C_6F_5Br^-$ (> 97% at 300 K and ~ 60% at 450 K) and Br$^-$ (< 3% at 300 K and ~ 40% at 450 K) with the percentage of Br$^-$ and the overall attachment rate coefficient, β, increasing with increasing temperature (see Table 1). The energetics for Br$^-$ and $C_6F_5^-$ production in this reaction are uncertain because there is not an accurate value of $D(C_6F_5-Br)$ available. A value of $D(C_6F_5-Br)$ — 105.9 kcal mol^{-1} has previously been reported [21] but this must be great'y in error since using this value, an endothermicity of 28.4 kcal mol^{-1} for Br$^-$ production is indicated and this cannot be remotely correct since Br$^-$ production is facile at 450 K in the FALP plasma. However an estimate of $D(C_6F_5-Br) \approx 80$ kcal mol^{-1} can be made by considering the trend in the analogous C_6H_5X compounds (where X — F, Cl, Br, and I) [15]

29

and this value along with the accurately known EA(Br) of 77.530 ± .092 kcal mol^{-1} has been used to calculate the ergicities of the following reactions:

$$C_6F_5Br + e \longrightarrow Br^- + C_6F_5 - \sim 3 \text{ kcal mol}^{-1} \text{ (est)} \qquad (3a)$$
$$\longrightarrow C_6F_5^- + Br - \sim 17 \text{ kcal mol}^{-1}\text{(est)} \qquad (3b)$$

Clearly the production of $C_6F_5^-$ is very endothermic and indeed is not observed in significant quantities in the FALP.

The appearance of $C_6F_5Br^-$ as the major product at 300 K in the FALP experiment is consistent with the long lifetime of the $(C_6F_5Br^-)^*$ ion determined by Naff et al [1], implying that this excited ion can be stabilized against autodetachment in collision with He atoms ($r_a \gg r_c$). Notwithstanding the fact that $(C_6F_5Br^-)^*$ ions can undergo collisions with He atoms during their lifetime, which may modify the nascent state distribution of the excited ions, we treat the product channels as separate reactions and, as before, assume a Boltzmann law to derive a ΔE for each reaction. Thus ΔE for Br^- production is calculated to be ~ 7 kcal mol^{-1}. As before this may represent a barrier to dissociative electron attachment or the endothermicity of the reaction and again these are indistinguishable. However, large barriers (> ~3 kcal mol^{-1}) to dissociative electron attachment are not uncommon [6,7] (note that the barrier for $C_6F_5^-$ production from C_6F_5I is approximately 2 kcal mol^{-1}). However, if the ΔE for Br^- production derived from the experiment represents an endothermicity of the reaction, then $D(C_6F_5-Br) = \Delta E + EA(Br) \cong 84$ kcal mol^{-1}. In view of the uncertainties as to whether ΔE represents an endothermicity or an activation energy barrier, this value should be viewed as an upper limit to $D(C_6F_5-Br)$. This upper limit is not inconsistent with the estimate of 80 kcal mol^{-1} obtained from the

analogous C_6H_5Br bond dissociation energy.

It is also interesting to note that an energy barrier of ~1.3 kcal mol^{-1} can be deduced for $C_6F_5Br^-$ production which is similar to the barrier for $C_6F_5Cl^-$ production mentioned previously. So it appears that the mechanism for parent ion production for C_6F_5Cl and C_6F_5Br are similar (C_6F_5I forms very little parent ion at 300 K).

CONCLUDING REMARKS

These studies of electron attachment to C_6F_5Cl, C_6F_5Br and C_6F_5I, have clearly shown how different product ions can result from electron attachment studied in a low pressure (beam) experiment in which the electrons are suprathermal in the ion source and in a "high" pressure experiment in which electrons are truly thermal. The production of $(C_6F_5I^-)^*$ in the FALP experiment but not in the t.o.f. experiment has been used to bracket the previously unknown lifetime to autodetachment, τ_a, of $(C_6F_5I^-)^*$ in the range $10^{-7}s < \tau_a (C_6F_5I^-)^* < 10^{-6}s$. It has also been shown that thermal electron attachment to C_6F_5Br yields both $C_6F_5Br^-$ and Br^-, from which an upper limit to $D(C_6F_5-Br)$ of ~84 kcal mol^{-1} has been established.

A most important conclusion to be drawn from these studies is that the rate coefficients and product ions resulting from attachment reactions of electrons with a given molecular species can be dependent on the environment in which the reaction occurs. Even where the electron/ molecule (M) interaction energies or temperatures are the same in two systems but where the ambient pressures are very different (such that the τ_c for collisions between the nascent parent negative ion $(M^-)^*$ and ambient gas atoms or molecules vary greatly relative to the autodetachment lifetime of $(M^-)^*$) then different results are to be

expected. Thus, for example, it is dangerous to assume that results obtained in very low pressure time-of-flight experiments and in low pressure experiments, including FALP results obtained at pressures of typically 1 torr, are appropriate to electron capture detectors which generally operate at ambient pressures close to atmospheric pressure. Recently, we observed that the CCl_3 radicals generated from the dissociation attachment reactions of CCl_4 with thermal electrons in the FALP plasma rapidly undergo dissociative attachment with thermal electrons [12]. However, we have been informed by Grimsrud [22] that he sees no evidence for such a phenomenon in his high pressure electron capture detectors. This difference may be a manifestation of the production of vibrationally-excited CCl_3 radicals in the CCl_4 + e dissociation attachment reactions which are not effectively quenched to the ground vibrational state before interacting with an electron in the lower pressure FALP but are quenched at the higher pressure of the capture detector. This would imply a barrier to dissociative attachment to CCl_3 radicals which is effectively overcome by vibrational excitation. More work is necessary to clarify this.

APPENDIX

Ion Molecule Reactions of $C_6F_5^-$

Little is known about the reactivity of $C_6F_5^-$ ions and so we chose to investigate this in order to gain a more complete understanding of the chemistry of this ionic species. Reactions of $C_6F_5^-$ with CH_3Cl, CH_3Br,

CH$_3$I, HF, HCl, HBr and C$_6$F$_5$Cl were studied at 300K using a selected ion flow tube (SIFT) apparatus which has been described in detail previously [23]. The carrier gas was pure helium at a pressure of about 0.5 torr. Copious amounts of C$_6$F$_5^-$ were produced by electron impact on C$_6$F$_5$I in a high pressure ion source and injected into the carrier gas. Reactant gas was added downstream and the binary rate coefficients, k$_2$, were determined in the usual manner [23]. The k$_2$ and the ionic products observed are listed in Table 2.

The k$_2$ for the reactions with CH$_3$Cl and HF (reactions (a) and (d) respectively in Table 2) were immeasurably small being $<10^{-13}$cm^{3}s^{-1}. This is not surprising for reaction (d) since it is calculated to be endothermic by about 6 kcal mol^{-1}. The reactions with CH$_3$Br and CH$_3$I (reactions (b) and (c)) seemingly occurr via a binary nucleophilic substitution mechanism [24, 25] (an S$_N$2 displacement mechanism [26]) giving Br$^-$ and I$^-$ as the product ions respectively. These reactions have small reaction efficiencies (k$_2$/k$_{ADO}$, where k$_{ADO}$ is the collisional limiting rate coefficient calculated using the average dipole orientation theory (ADO) [27]; see Table 2). Many organic ion-molecule reactions proceed with k$_2$ well below their collisional limiting values, this being qualitatively ascribed to the effect of a double-well potential surface [24, 28]. However, it is interesting to note that in reactions (a) to (c) the nucleophile, C$_6$F$_5^-$, and the substrate, CH$_3$, are obviously the same and thus the leaving group ability of the halogen ion should be an important factor affecting the efficiency of the reactions. It is known that the leaving group abilities of the halogen ions in the gas phase are the same as in the liquid phase, i.e. I$^-$>Br$^-$>Cl$^-$ and, as can be seen from Table 2, the efficiencies of reactions (a)-(c) do indeed increase with the leaving group abilities of the halogen ions. Note also that the reaction efficiency increases with the exothermicity of the reactions.

The reactions with HCl and HBr (reactions (e) and (f) in Table 2) giving Cl^- and Br^- as product ions are proton transfer reactions and proceed with k_2 which are appreciable fractions of, although significantly smaller than, their collisional limiting values. Proton transfer to negative ions generally occurs at or near the collisional limiting value for localised anions (e.g., O^-, OH^- and C_2H^-)[29]. However there are many examples of relatively slow proton transfer for delocalised anions (e.g., $C_6H_5O^-$ and $(C_6H_5)CH_2^-$) [28]. $C_6F_5^-$ is a delocalised anion and thus it is not surprising that the k_2 for reactions (e) and (f) are significantly smaller than their collisional limiting values.

The reaction with C_6F_5Cl (reaction (g)) proceeds with a k_2 of $1.9 \times 10^{-10} cm^3 s^{-1}$ which again is significantly smaller than the collisional value and as before the halogen negative ion is the product. (Since the polarizability of C_6F_5Cl is unknown, k_{ADO} could only be estimated as $5.2 \times 10^{-10} cm^3 s^{-1}$ (using an estimated polarizability of $5 \times 10^{-24} cm^3$) giving a reaction efficiency of 0.3). This reaction probably proceeds via an addition elimination mechanism [30], with the strong electron withdrawing F atoms stabilizing the resulting carbanion which then eliminates Cl^- to produce $(C_6F_5)_2$. Dissociative charge transfer from $C_6F_5^-$ to C_6F_5Cl to give Cl^- and two C_6F_5 radicals is not possible since this process is ~55 kcal mol^{-1} endothermic. The relative inefficiency of this reaction may be attributed to a barrier on an, as yet, undetermined potential surface.

REFERENCES

1. W.T. Naff, R.N. Compton and C.D. Cooper, *J. Chem. Phys.* 54 (1971) 212.

2. R.L, Woodin, M.S. Foster and J.L. Beauchamp, *J. Chem. Phys.* 72 (1980) 4223

3. A. Chutjian and S.H. Alajajian, *Phys. Rev.* 131 (1985) 2885.

4. L.M. Chanin, A.V. Phelps and M.A. Biondi, *Phys. Rev. Lett.* 2 (1959).

5. R.W. Crompton and G.N. Haddad, *Aust. J. Phys.*, 36, (1983) 15.

6. E. Alge, N.G. Adams and D. Smith, *J. Phys. B. At. Mol. Phys.* 16 (1983) 1433.

7. D. Smith, N.G. Adams, and E. Alge, *J. Phys. B. At. Mol. Phys.* 17 (1984) 461.

8. N.G. Adams, D. Smith, E. Alge and J. Burdon, *Chem. Phys. Letters* 116 (1985) 460.

9. S.M. Spyrou and L.G. Christophorou, *J. Chem. Phys.* 82 (1985) 1048.

10. N. Herdandex-Gil, W.E. Wentworth, T. Limeru, and E.C.M. Chen, *J. Chromatogr.* 312 (1984) 31.

11. L.G. Christophorou, *J. Chem. Phys.* 83 (1985) 6543.

12. N.G. Adams, D. Smith and C.R. Herd, *Int. J.Mass. Spectrom. and Ion Processes* 84 (1988) 231.

13. I. Dimicolli and R. Botter, *J. Chem. Phys.* 74(4) (1981) 2355.

14. R.W. Marawar, C.W. Walter, K.A. Smith and F.B. Dunning, *J. Chem. Phys.* 88(4) (1988) 2853.

15. T.M. Miller, CRC Handbook of Chemistry and Physics, 66th edition CRC Press, Inc. Boca Raton, FL., E-62.

16. F.M. Page and G.C. Goode, in : Negative Ions and the Magnetron, Wiley-Interscience, New York, 1969.

17. R.N. Compton and P.W. Reinhardt, *Chem. Phys. Letters*, 91 (1982) 268.

18. M.J. Kreech, S.J.W. Price and W.F. Yared, *Int. J. Chem. Kinetics*, **6** (1974) 257.

19. C.E. Klots, *Chem. Phys. Lett.*, **38** (1976) 61.

20. K.Y. Choo, O.M. Golden, and S.W. Benson, *Int. J. Chem. Kinet.*, **7**, (1975) 713.

21. S.J.W. Price and H.J. Sapiano, *Can. J. Chem.*, **52** (1974) 4109.

22. E. Grimsrud, private communication.

23. D. Smith and N.G. Adams in M.T. Bowers (Ed.), Gas Phase Ion Chemistry, Vol.1, Academic Press, New York, 1979, p.1; D. Smith and N.G. Adams in D. Bates and B. Bederson (Eds.), *Advances in Atomic and Molecular Physics*, Vol. 24, Academic Press, New York, 1988 in press.

24. W.N. Olmstead and J.I. Brauman, *J. Am. Chem. Soc.* **99** (1977) 4219.

25. M. Tanaka, G.I. Mackay, J.D. Payzant, and D.K. Bohme, *Can. J. Chem.* **54** (1976) 1643.

26. T.H. Lowry and K.S. Richardson, *Mechanism and Theory in Organic Chemistry*, Harper and Row Publishers Inc. New York (1976).

27. T.Su and M.T. Bowers in Gas Phase Ion Chemistry, Vol 1, M.T. Bowers, Ed., Academic Press, New York (1979) p.83.

28. W.E. Farneth and J.I. Brauman, *J. Am. Chem. Soc.*, **98**(5) (1976), 7891.

29. D.K. Bohme in Interactions Between Ions and Molecules, P. Ausloos, Plenum Press, New York 1975 pp. 489-504.

30. J.M. Harris and C.S. Wamser, Fundamentals of Organic Reaction Mechanisms, John Wiley and Sons, Inc. New York, 1976.

31. T. Su and M.T. Bowers, *Int. J. Mass Spectrom. Ion Phys.* **12** (1973) 347.

32. T. Su and M.T. Bowers, *Int. J. Mass Spectrom. Ion Phys.* **17** (1975) 211.

TABLE 1

Rate Coefficients and Product Ion Distributions for Electron Attachment to C_6F_5Cl, C_6F_5Br, and C_6F_5I

Reaction	Temperature = 300K		Temperature = 450K	
	β (cm^{3}s^{-1})	ion products	β (cm^{3}s^{-1})	ion products
$C_6F_5Cl + e$	4.9×10^{-8}	$C_6F_5Cl^-$ (100)	1.0×10^{-7}	$C_6F_5Cl^-$ (100)
$C_6F_5Br + e$	6.1×10^{-8}	$C_6F_5Br^-$ (≥ 97) Br^- (≤ 3)	2.0×10^{-7}	$C_6F_5Br^-$ (~ 60) Br^- (~ 40)
$C_6F_5I + e$	3.2×10^{-8}	$C_6F_5^-$ (≥ 95) $C_6F_5I^-$ (≤ 5)	1.1×10^{-7}	$C_6F_5^-$ (~ 100) I^- (trace)

TABLE 2

Rate coefficients, k_2, at 300K for the reactions of $C_6F_5^-$ with the molecules indicated as measured using a selected ion flow tube (SIFT). Also listed are the collisional limiting values of the rate coefficients k_{ADO}, the reaction efficiences (k_2/k_{ADO}) and the reaction ergicities ΔH_r (calculated from the bond dissociation energies and electron affinities given in ref. 15). The polarizabilities and dipole moments of the neutral molecules which were required to calculate k_{ADO} were obtained from ref. 15 and the dipole locking constants were determined from data in refs. 31 and 32.

Reaction	$k_2(cm^3s^{-1})$	$k_{ADO}(cm^3s^{-1})$	k_2/k_{ADO}	$\Delta H_r(kcal\ mol^{-1})$
a. $C_6F_5^-+CH_3Cl$: no reaction	$<10^{-13}$	1.40×10^{-9}	7.0×10^{-5}	-41
b. $C_6F_5^-+CH_3Br\longrightarrow C_6F_5CH_3+Br^-$	4.4×10^{-12}	1.14×10^{-9}	3.9×10^{-3}	-49
c. $C_6F_5^-+CH_3I\longrightarrow C_6F_5CH_3+I^-$	6.5×10^{-11}	1.04×10^{-9}	6.3×10^{-2}	-57
d. $C_6F_5^-+HF$: no reaction	$<10^{-13}$	1.79×10^{-9}	5.6×10^{-5}	$+6$
e. $C_6F_5^-+HCl\longrightarrow C_6F_5H+Cl^-$	6.0×10^{-10}	1.05×10^{-9}	5.7×10^{-1}	-41
f. $C_6F_5^-+HBr\longrightarrow C_6F_5H+Br^-$	2.0×10^{-10}	7.44×10^{-10}	2.7×10^{-1}	-41
g. $C_6F_5^-+C_6F_5Cl\longrightarrow (C_6F_5)_2+Cl^-$	1.9×10^{-10}	-	-	-45

APPENDIX 3

MEASUREMENTS OF THE DISSOCIATIVE RECOMBINATION COEFFICIENTS FOR

SEVERAL POLYATOMIC SPECIES AT 300K

N.G. ADAMS and D. SMITH

MEASUREMENTS OF THE DISSOCIATIVE RECOMBINATION COEFFICIENTS
FOR SEVERAL POLYATOMIC ION SPECIES AT 300 K

Nigel G. ADAMS and David SMITH

Department of Space Research, University of Birmingham, Birmingham B15 2TT, UK

The dissociative recombination coefficients, α, have been measured at 300 K for several polyatomic positive ion species using a flowing afterglow/Langmuir probe (FALP) apparatus. The α range from 1.1×10^{-7} cm^3 s^{-1} for H_2F^+ to 2.2×10^{-6} cm^3 s^{-1} for the clustered species $H^+(CH_3OH)_3$. Several of the ionic species included in this study are considered to be involved in the synthesis of interstellar molecules.

1. Introduction

Electron–positive ion dissociative recombination is an important loss process in gaseous plasmas in which significant fractions of the ions are molecular. The dissociative recombination coefficients, α, for the reactions of a number of diatomic, triatomic and polyatomic species with electrons have been determined using a variety of techniques, including the collision-dominated stationary afterglow technique [1] and the merged (ion–electron) beam technique [2]. The flowing afterglow/Langmuir probe (FALP) technique, developed in our laboratory, is well suited to the determination of α over the temperature range 90–600 K (the actual range being limited by condensation or decomposition of vapours used to create the ions) for any positive ion species which can be created as the dominant ion in the flowing afterglow plasma. The well-known chemical versatility of the flowing afterglow, which has been demonstrated principally by numerous studies of ion–molecule reactions [3], has provided the opportunity to determine the α for many ionic species, including NO$^+$ and O$_2^+$ [4], and a few simple interstellar ion species, including HCO$^+$, N$_2$H$^+$ and CH$_5^+$ [5,6]. During the latter measurement programme, we also observed that, contrary to previously published work, H$_3^+$ ions do not rapidly dissociatively recombine with electrons. Indeed, the H$_3^+$ recombination coefficient, $\alpha(H_3^+)$, was too small to be measured in the FALP

[5]. This observation has considerable significance to interstellar chemistry because of the central role which H$_3^+$ ions play in that chemistry [7–9]. From a practical viewpoint, this observation is also important in that it provides the opportunity to study α for a wide range of ionic species in the FALP by the following method. It is simple to create H$_3^+$ / electron afterglow plasmas since these do not decay significantly by recombination. Because protons are readily transferred from H$_3^+$ to most molecular species (a consequence of the small proton affinity, PA, of H$_2$), then the addition of a sufficient concentration of a molecular species, X, to a H$_3^+$/electron afterglow will create a plasma consisting of XH$^+$ ions and electrons following the reaction

$$H_3^+ + X \rightarrow XH^+ + H_2 . \tag{1}$$

Such reactions are always rapid when PA(X) exceeds PA(H$_2$), as is the case for many molecular species, X. Thus, we have exploited this process in the present study to determine the α for a number of molecular ions using the FALP. Several of the molecular ions included in this study are considered to be involved in interstellar molecular synthesis.

2. Experimental

The FALP technique has been described in detail previously [4,10,11]. It has been used successfully

11

to determine ion–ion recombination coefficients [12] and electron attachment coefficients[11,13] as well as electron–ion recombination coefficients [4,5]. For the last mentioned studies, a microwave discharge is created upstream in flowing helium carrier gas at a pressure of about 1 Torr. The afterglow formed downstream contains metastable helium atoms, He^m, and He_2^+ ions (formed by the ternary association of He^+ ions with He atoms). The addition of sufficient argon downstream of the discharge (but upstream of the reaction zone where recombination is to be observed) destroys both the He^m and He_2^+, thus producing Ar^+ ions. The addition of H_2 to the Ar^+/electron afterglow plasma rapidly converts the Ar^+ to ArH^+, which then reacts rapidly with H_2 thus forming a non-recombining H_3^+/electron afterglow plasma. In this plasma, loss of electrons occurs only via the slow process of ambipolar diffusion as is readily demonstrated by measuring the reduction in the electron density, $n_e(z)$, with distance z, along the axis of the flow tube using a movable Langmuir probe, which is the primary diagnostic tool in the FALP. The addition of a gas or vapour, X, results (according to eq. (1)) in the rapid creation of a recombining plasma consisting of XH^+ ions and electrons. This is manifest by an increase in the gradient in $n_e(z)$ immediately downstream of the inlet port through which X is introduced (i.e. in the reaction zone). This port is located 57.5 cm from the sampling point of the downstream quadrupole mass filter which is used to identify the ion types present in the plasma. It is then a simple matter to analyse the $n_e(z)$ data to determine α for the XH^+ ions in the afterglow plasma. Since diffusive loss can be ignored,

$$v_p \, \partial n_e/\partial z = -\alpha n_e(z) \, n_+(z) , \qquad (2)$$

where the XH^+ number density, $n_+(z) = n_e(z)$ in the quasi-neutral plasma, and v_p is the plasma flow velocity which is readily determined as described in a previous paper and is typically $10^4 \, cm^3 \, s^{-1}$ [14]. The continuity equation (2) is readily integrated and indicates that a plot of $n_e^{-1}(z)$ against z should be linear with a slope equal to α/v_p. All the α reported below were obtained using this analytical approach at a helium carrier gas temperature of 300 K.

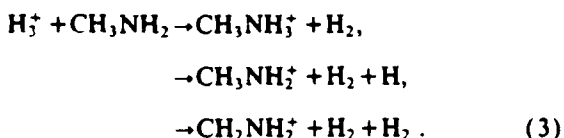## 3. Results

A wide variety of molecules, X, were chosen for this study, these varying in complexity from HF to C_2H_5OH. Thus, the α for the corresponding protonated molecules XH^+, i.e. H_2F^+, $C_2H_5OH_2^+$, etc. were determined at 300 K. Fortunately, the rate coefficients and product ions for the reactions of H_3^+ with the majority of the molecular species X included in this work (table 1) had been studied previously [15] and these data were a helpful guide in understanding the chemistry involved in the production of the recombining FALP plasmas. For the H_3^+ reactions which had not been studied previously (i.e. for $X = HF$, CH_3C_2H, CH_3SH, C_2H_5OH and CH_3NH_2), we measured the rate coefficients at 300 K in a parallel selected ion flow tube (SIFT) study. All five reactions proceeded rapidly, the rate coefficients, $k(X)$, being close to the respective collisional rate coefficients.
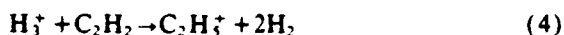
The terminating ions of most of these primary $H_3^+ + X$ reactions (and any subsequent secondary reactions of the primary product ions with X) are the protonated ions XH^+ (except for the reaction involving CH_3C_2H which results in a mixture of $C_3H_5^+$ and $C_6H_5^+$; see table 1). For some X, the proton-transfer reaction with H_3^+ is sufficiently exothermic (i.e. $PA(X) \gg PA(H_2)$) that dissociative proton transfer and other chemistry occur, e.g.

Table 1

Dissociative recombination coefficients measured at 300 K using the FALP

Recombining ion	Recombination coefficient, α ($cm^3 \, s^{-1}$)	Source gas, X
H_2F^+	1.1(−7)	HF
HCO_2^+	3.4(−7)	CO_2
$C_3H_5^+/C_6H_5^+ \approx 1/1$	3.5(−7)	CH_3C_2H
H_2CN^+	3.5(−7)	HCN
H_3S^+	3.7(−7)	H_2S
HN_2O^+	4.2(−7)	N_2O
$C_4H_5^+$	6.2(−7)	C_4H_2
$C_2H_5^+$	7.4(−7)	C_2H_6
$CH_3SH_2^+$	7.7(−7)	CH_3SH
HCS^+	9.1(−7)	CS_2
$CH_3NH_3^+$	1.4(−6)	CH_3NH_2
$H^+(CH_3OH)_{1,2,3}$	8.8(−7)→2.2(−6)	CH_3OH
$H^+(C_2H_5OH)_{1,2,3}$	1.1(−6)→1.9(−6)	C_2H_5OH

12

$$H_3^+ + CH_3NH_2 \rightarrow CH_3NH_3^+ + H_2,$$

$$\rightarrow CH_3NH_2^+ + H_2 + H,$$

$$\rightarrow CH_2NH_2^+ + H_2 + H_2 . \tag{3}$$

However an excess of CH_3NH_2 ensures that secondary reactions occur, generating $CH_3NH_3^+$ as the terminating ion in the plasma. Also the H_3^+ reaction with C_2H_6 proceeds thus,

$$H_3^+ + C_2H_2 \rightarrow C_2H_3^+ + 2H_2 \tag{4}$$

and, since the rate coefficient for the subsequent reaction of the product ion $C_2H_3^+$ with C_2H_6 is small, the $\alpha(C_2H_3^+)$ could be determined. On addition of C_2H_2 to the H_3^+ plasma, rapid primary and secondary reactions led to $C_4H_3^+$:

$$H_3^+ + C_2H_2 \rightarrow C_2H_3^+ + H_2 \tag{5}$$

$$C_2H_3^+ + C_2H_2 \rightarrow C_4H_3^+ + H_2 , \tag{6}$$

allowing $\alpha(C_4H_3^+)$ to be obtained but not $\alpha(C_2H_3^+)$.

The α which have been determined in this study are given in table 1 and the gases or vapours, X, from which the ions were generated are indicated. To our knowledge, the α for these recombination reactions have not been determined previously and so comparisons cannot be made. The measured α are considered to be accurate to $\pm 25\%$. For the mixture $C_3H_3^+/C_6H_5^+$ ions (in approximately equal concentrations) a "mean α" is all that could be obtained. However, if the α values for $C_3H_3^+$ and $C_6H_5^+$ had been greatly different from each other then this would have been apparent as a curvature of the plots of n_e^{-1} against z (referred to in section 2). Mean α are also given in table 1 for the protonated clusters of CH_3OH and C_2H_5OH. The smallest value of α in each case refers to the protonated ("core") ions $CH_3OH_2^+$ and $C_2H_5OH_2^+$. As the flow rates (number densities) of the CH_3OH and C_2H_5OH were increased in the plasma afterglow, clustering of the parent molecules to the "core" ions occurred (as indicated by the mass spectrometer) and the derived α increased as a result by a factor of two to three. The largest value of α in each case indicates the *lower limits* to the α for the cluster ions $H^+(CH_3OH)_3$ and $H^+(C_2H_5OH)_3$. Increases in α by similar factors have been observed previously for the clustering of H_2O ligands to H_3O^+ [16] and NH_3 ligands to NH_4^+ [17].

The α in table 1 are arranged vertically in order of increasing magnitude so that it can be seen that there is a general trend towards an increasing magnitude of α with increasing complexity (atomicity) of the recombining ion, as previous work has also indicated [18]. However, this is by no means a "golden rule" and each recombining system should be considered independently (note, for example, that $\alpha(CH_5^+) = 1.1 \times 10^{-6} \text{ cm}^3 \text{ s}^{-1}$ at 300 K [5,6], which exceeds $\alpha(CH_3OH_2^+)$, see table 1). These are unique recombination data which will find applications in calculations of deionization rates for laboratory plasmas and especially for dense interstellar cloud chemistry.

Acknowledgement

References

[1] F.J. Mehr and M.A. Biondi, Phys. Rev. 181 (1969) 264.

[2] D. Auerbach, R. Cacak, R. Caudano, T.D. Gaily, C.J. Keyser, J.Wm. McGowan, J.B.A. Mitchell and S.F.J. Wilk, J. Phys. B10 (1977) 3797.

[3] N.G. Adams and D. Smith, in: Techniques for the study of gas-phase ion–molecule reactions, eds. J.M. Farrar and W.H. Saunders Jr. (Wiley-Interscience, New York, 1988), to be published.

[4] E. Alge, N.G. Adams and D. Smith, J. Phys. B16 (1983) 1433.

[5] N.G. Adams, D. Smith and E. Alge, J. Chem. Phys. 81 (1984) 1778;
N.G. Adams and D. Smith, in: Astrochemistry, eds. M.S. Vardya and S.P. Tarafdar (Reidel, Dordrecht, 1987) pp. 1–18.

[6] D. Smith and N.G. Adams, Astrophys. J. 284 (1984) L13.

[7] A. Dalgarno and J.H. Black, Rept. Progr. Phys. 39 (1976) 573.

[8] D. Smith and N.G. Adams, Intern. Rev. Phys. Chem. 1 (1981) 271.

[9] D. Smith, Phil. Trans. Roy. Soc. (London) (1987), to be published.

[10] D. Smith and N.G. Adams, in: Physics of ion–ion and electron–ion collisions, eds. F. Brouillard and J.W. McGowan (Plenum Press, New York, 1983) pp. 501–531

13

[11] D. Smith, N.G. Adams and E. Alge, J. Phys. B17 (1984) 461.

[12] D. Smith, M.J. Church and T.M. Miller, J. Chem. Phys. 68 (1978) 1224.

[13] E. Alge, N.G. Adams and D. Smith, J. Phys. B17 (1984) 3827.

[14] N.G. Adams, M.J. Church and D. Smith, J. Phys. D8 (1975) 1409.

[15] V.G. Anicich and W.T. Huntress Jr., Astrophys. J. Suppl. Ser. 62 (1986) 553.

[16] M.T. Leu, M.A. Biondi and R. Johnsen, Phys. Rev. A7 (1973) 292.

[17] C.M. Huang, M.A. Biondi and R. Johnsen, Phys. Rev. A14 (1976) 984.

[18] M.A. Biondi, Comments At. Mol. Phys. 4 (1973) 85.

14

APPENDIX 4

FALP STUDIES OF POSITIVE ION/ELECTRON RECOMBINATION

N.G. ADAMS and D. SMITH

Proceedings of a Symposium on 'Electron/Ion Recombination'

held at Lake Louise, Canada, June 1988

Eds. J.B.A. Mitchell and S.L. Guberman

World Publ. Co., in press

FALP STUDIES OF POSITIVE ION/ELECTRON RECOMBINATION

Nigel G. Adams and David Smith

Department of Space Research

University of Birmingham

Birmingham, B15 2TT, UK.

ABSTRACT. The application of the Flowing Afterglow /Langmuir Probe (FALP) technique to the study of positive ion/electron recombination is described. Measurements of the dissociative recombination coefficients, α, for O_2^+ and NO^+ have demonstrated that the FALP technique is reliable. Detailed studies of H_3^+/electron flowing afterglow plasmas have shown that no measurable recombination of ground vibrational state H_3^+ ions occurs and that $\alpha(H_3^+) \lesssim 2 \times 10^{-8} cm^3 s^{-1}$. Subsequently, this upper-limit value for $\alpha(H_3^+)$ has been considerably lowered by comparing the loss rate of the H_3^+ ions with that of atomic He^+ ions. The FALP values of $\alpha(H_3^+)$ are much smaller than those obtained using some other techniques and reasons are given for the differences. Addition of a molecular gas, X, to the non-recombining H_3^+/electron flowing afterglow plasma generally results in the production of a plasma comprising XH^+ ions and electrons which invariably undergoes recombination. Thus the α for several XH^+ ion species have been determined, some over appreciable temperature ranges, including species for which X = CO, N_2, H_2O, CH_4 and CH_3OH. Work is now in progress to identify the neutral products of some dissociative recombination reactions. With this objective in mind, both vacuum ultraviolet and laser induced fluorescence spectroscopy are being applied to the determination of the neutral fragments of recombination reactions. Preliminary results concerning H_3O^+ recombination are reported.

INTRODUCTION

Positive ion/electron recombination processes are important in controlling the degree of ionization in most types of ionized gases and plasmas. Radiative, dielectronic, collisional-radiative, collisional and dissociative recombination are well-characterized processes, and which of these processes occurs or dominates the ionization loss in a particular plasma depends on the physical and chemical properties of the plasma, i.e. the number densities of ions and electrons, the kinetic temperatures of the charged species and the nature of the ions. Thorough discussions of these various recombination processes have been given in some authoritative texts[1-4]. Plainly, dissociative recombination can only occur in ionized media containing molecular ions. However, this encompasses most laboratory plasmas (except the very high temperature fusion plasmas in which all primary molecular gases are fully dissociated and ionized) and many naturally-occurring plasmas such as the terrestrial ionosphere and interstellar gas clouds. A proper understanding of the ion chemistry of such media and the equilibrium degree of ionization (controlled by the balance between the ionization rate and recombination rate) demands a knowledge of the rate coefficients for dissociative recombination reactions, α, the variations of the α with temperature, and the identity of the neutral products of the reactions, often for a considerable number of different positive ion species.

The physical conditions under which recombination occurs have a controlling influence on the rate of recombination, and thus experiments designed to study recombination, in order to provide data to be used to facilitate ion chemical models of ionized media, should attempt to simulate the conditions pertaining to the ionized media of interest as far as possible. Accurate laboratory simulation of the physical conditions is not practically possible for media such as the ionosphere (low ionization density, unequal electron and ion temperatures, solar radiation field which influences the internal states of the recombining ions, etc.)[5,6] and interstellar gas clouds (very low ionization density, very low temperatures)[7,8]. However, using afterglow plasma techniques, recombination can be studied at temperatures not greatly different from

those appropriate to the above media, although the ionization density and the neutral gas density are necessarily much greater in order to enhance the recombination loss relative to diffusion loss[2,9] and this difference must be considered when utilizing such laboratory data in ion-chemical models of naturally-occurring plasmas. A definite advantage in studying dissociative recombination at relatively high gas number densities is that the recombining molecular ions undergo multiple collisions with ambient atoms and/or molecules prior to their recombination with the electrons which assists in removing any nascent internal excitation. Then it can usually be assumed with confidence that the ions under study are in their ground rovibronic states.

On the other hand, a disadvantage of a relatively high gas pressure is that it can catalyse the production of "cluster ions" (i.e. the bonding of ligand molecules to the "core ions" which are to be studied) especially at low temperatures. Since the recombination coefficients for "cluster ions" are often much greater than for the simple "core ions"[10] then the presence of even small fractions of cluster ions can enhance the loss rate of electrons from the plasma and lead to erroneous values of the α for the "core ions". The low pressure, essentially collisionless merged beam method for studying recombination processes effectively circumvents this problem and can provide data on the cross sections, σ, for the dissociative recombination of a very wide variety of mass analysed positive ions[11]. However, although such data are of great value to the understanding of the fundamental nature of the recombination process, they are not directly applicable to models of low temperature media because the interaction energy of the ions and electrons, and hence the rate coefficients for recombination, cannot be ascertained sufficiently accurately at the very low interactions energies necessary. Also the degree of internal excitation of the ions is often uncertain in merged beam experiments, although this is presumably not a fundamental limitation since ion source developments should enable such problems to be minimised[12].

The strengths and limitations of merged beam methods and afterglow methods have been discussed in previous research papers and reviews and

47

so they will not be given here[4,9,13]. In this paper, we are entirely concerned with the application of the flowing afterglow/Langmuir probe (FALP) method developed in our laboratory to the study of positive ion/electron recombination reactions, especially dissociative recombination reactions, of ions considered to be involved in atmospheric and interstellar ion chemistry.

THE FALP EXPERIMENT

In a continuous electrical discharge through a gas, the mean energies or "temperatures" of the electrons and ions, especially the electrons, are inevitably greater than the neutral gas temperatures by virtue of the energy that the charged particles gain from the electric field sustaining the discharge. When the electric field is removed the temperatures of the charged particles relax to that of the ambient neutral gas and an afterglow plasma may be formed in which the temperatures of charged and neutral particles are equal. Reactions between the composite particles of the afterglow plasma can then be studied under thermalised conditions. This is the basis of the time-resolved or stationary afterglow (SA) technique which has been exploited for many years by Biondi and his colleagues to determine dissociative recombination coefficients for a wide variety of molecular positive ion species. This pioneering work has been described in several reviews (see, for example, references 2) and 10)). The SA has also been used to great effect to study diffusion processes[14] and ion-neutral reactions [15]. However, the SA method is limited in its scope because reactant ions must be formed by subjecting a pure gas or, more generally, a gas mixture to an electrical discharge. This usually generates more than one ionic species and sometimes internally excites the neutral gas (or gases) which creates great problems of data interpretation and can lead to erroneous results.

With the advent of the flowing afterglow (FA) method, these problems have been circumvented[16,17]. In this method, ionization is created by a continuous electrical discharge or some other form of ion source in the upstream region of a carrier gas (usually pure helium at about 1 torr) which is constrained to flow rapidly along a flow tube (about 1m long and

10cm diameter) by the action of a large mechanical (Roots-type) pump. A flowing afterglow plasma is thus created along the flow tube in which the temperatures of the charged particles have relaxed to the carrier gas temperature by the time they reach the downstream region. Gases can now be introduced into this thermalised plasma to create plasmas of different ionic composition as a result of the reactions of the added gases with the ambient ions and/or helium metastable atoms. Thus, for example, the addition of sufficient O_2 to the helium afterglow (comprised of He^+, He_2^+ ions, triplet He metastable atoms and electrons at number densities of the order of 10^8 - $10^{11}cm^{-3}$, and ground state helium atom number densities of about $(2-4) \times 10^{16}cm^{-3}$ at 300K) results in the production of an O_2^+/electron afterglow plasma. By controlling the flow rate of the reactant gas (O_2 in this case) into the afterglow and monitoring the number density of the reactant ions (e.g. He^+) in the plasma utilizing a *downstream mass-spectrometer/detection system*, the rate coefficient for the ion-molecule reaction and the ion products of the reaction can be determined. The critical point is that the reactant gas is not subjected to the electrical discharge (as it is in the SA) and so it is not significantly internally excited. Sequential additions of gases along the flowing afterglow produce sequential ion-neutral reactions and thus the technique has great chemical versatility.

The FA was originally used to determine the rate coefficients for a large number of ion-neutral reactions, some over wide temperature ranges, and this has led to the characterization of several ion-neutral reaction processes and also to the elucidation of the ion chemistry of the ionosphere[18]. However, in recent years it has been largely replaced by the selected ion flow tube (SIFT) method for the study of ion-neutral reactions[17,19,20].

A new application of the FA arose following the development of the single Langmuir probe technique to measure electron and ion number densities and electron temperatures in stationary afterglow plasmas[21]. It was a natural development to unite the probe diagnostic method and the FA and this created the flowing afterglow/Langmuir probe (FALP) apparatus with which several different types of plasma reaction processes can be

studied. The FALP technique has been described in detail previously[9,22] and therefore will only be alluded to here. A small cylindrical Langmuir probe (a tungsten wire approximately 0.5 cm long and 25 μm diameter) can be positioned at any point along the afterglow plasma axis. The potential of the probe is swept by $\pm$ 2 volts relative to the stainless steel walls of the flow tube and the current flowing to the probe from the plasma is measured. In this way, a current/voltage characteristic is obtained for the probe/plasma system which is analysed by a microcomputer and thus the electron number density (n_e) , ion number density (n_+) and electron temperature (T_e) can be readily obtained at any position (z) along the axis of the thermalised plasma.

In the pure helium plasma, diffusion of electrons and ions is the only loss process and from a measurement of n_e versus z, the ambipolar diffusion coefficient can be determined. The addition of small amounts of argon to the afterglow plasma results in the destruction of helium metastable atoms and the production of Ar^+ ions by Penning reactions. This is a convenient way of removing metastables, which could otherwise be a source of ionization in the downstream afterglow following the addition of reactant gases.

To determine the dissociative recombination coefficient, α, for a particular positive ion species, it is necessary to create an afterglow plasma ideally comprising only that ionic species and electrons. This is possible for a large variety of species because of the chemical versatility of the FA, although small fractions of unwanted ionic species are sometimes unavoidably present and then these species have to be accounted for in the analysis of data and the derivation of the α. The first α to be determined using the FALP method was that for O_2^+, i.e. $\alpha(O_2^+)$[23]. The O_2^+/electron plasma was created in the downstream region by the addition of O_2 to the helium afterglow as mentioned above. In the region of the afterglow upstream of the O_2 addition point, the gradient of n_e with z was small and, as expected, characteristic of diffusive loss of ionization, but downstream of the O_2 addition point, the gradient of n_e was much steeper indicating the occurrence of the additional loss process of dissociative recombination of O_2^+ ions with electrons (see
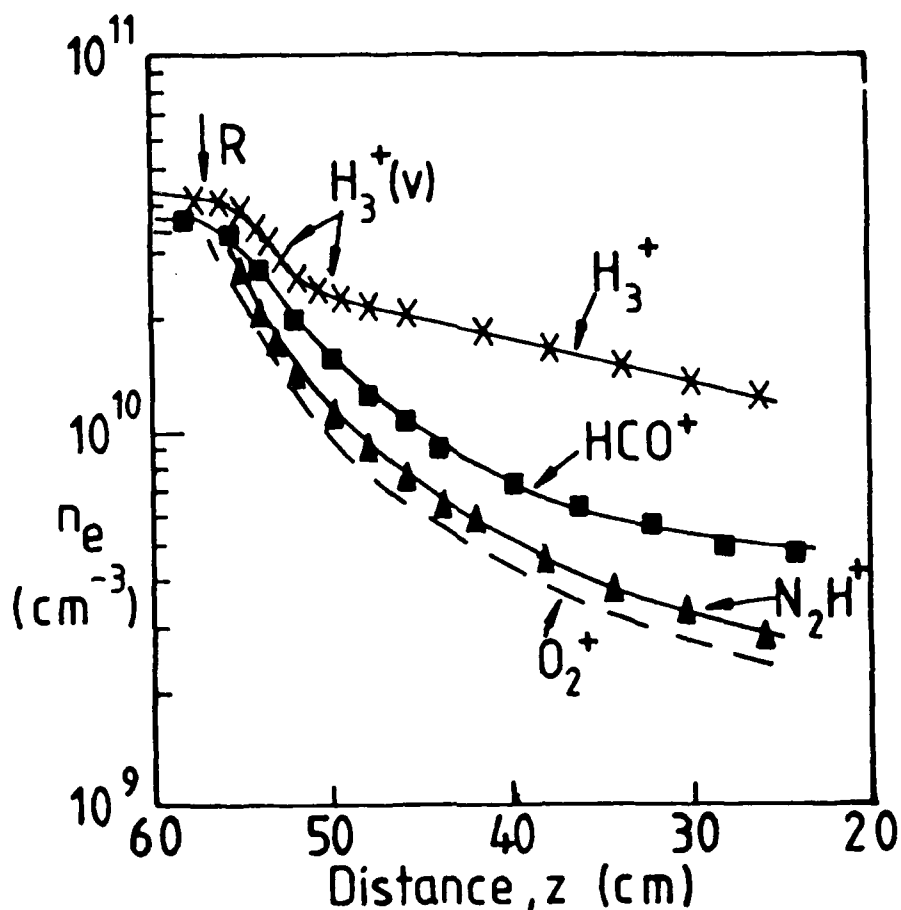
Fig.1.   A sample of data obtained from the FALP experiment.   The reduction of the electron number density, n_e, with distance along the plasma column, z, is very gradual upstream of the entry port, R, through which gases are added to form molecular ions in the afterglow plasma. On addition of H_2 at R, an obvious increase in the loss rate of electrons from the plasma occurs which is due to recombination of vibrationally excited H_3^+ ions.   Subsequently, the linearity of the log n_e versus z plot is characteristic of electron and ground state H_3^+ ion loss by ambipolar diffusion and not by recombination.   The addition of small amounts of CO or N_2 to the H_3^+ plasma creates HCO^+ and N_2H^+ plasmas.   The relatively rapid reduction of n_e with z in these plasmas is a manifestation of dissociative recombination of HCO^+ and N_2H^+ ions with electrons.   Electron loss by recombination in an O_2^+ plasma is also shown (see text).
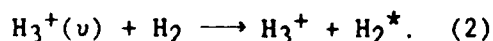
Fig. 1). Under conditions for which diffusive loss is small relative to recombination loss, i.e. high n_e to enhance recombination and high carrier gas pressure to inhibit diffusion, then a plot of n_e^{-1} versus z is linear and the slope of the plot is equal to α/v_p , where v_p is the flow velocity of the plasma (a parameter which is readily determined[24]). The $\alpha(O_2^+)$ at 300K determined in this way is in excellent agreement with those obtained previously by several other workers using different techniques [25]. (A measurement of $\alpha(O_2^+)$, and indeed $\alpha(NO^+)$ which is also now well known[23,26], is an excellent way of calibrating any system to be used to determine dissociative recombination coefficients.) The temperature of the FALP apparatus can be varied over the approximate temperature range of 90 to 600K, and so α values can be determined over this temperature range for a wide variety of positive ion species (Note that problems can arise due to condensation of vapours at the lower temperatures and this restricts the temperature range over which the α can be determined for some ions). The first paper reporting FALP measurements of α included those for O_2^+, NO^+, and NH_4^{+}[23]. These data illustrated that when the α are relatively small at 300K (i.e. between 10^{-7} and $10^{-6} cm^3 s^{-1}$) then they varied significantly with T (e.g. $\alpha(O_2^+)$ $\sim T^{-0.7}$; $\alpha(NO^+)$ $\sim T^{-0.9}$) whereas when α is large at 300K (i.e. $>10^{-6} cm^3 s^{-1}$) then the variation with T is less marked, as is the case for both H_3O^+ and NH_4^+ [23,27]. This feature of recombination reactions had been revealed previously by SA studies[28,29].

STUDIES OF H_3^+ RECOMBINATION

H_3^+ ions are formed in ionized gases rich in H_2 via the reaction of H_2^+ ions with H_2.

$$H_2^+ + H_2 \longrightarrow H_3^+(v) + H \tag{1}$$

It has been established experimentally that the H_3^+ ions formed in this reaction are vibrationally excited (the vibrational distribution peaking at $v=3$ or 4)[30,31]. It is also known that the $H_3^+(v)$ ions are relaxed to their ground vibrational states in collisions with H_2 (via the process of proton transfer)[30-32].

$$H_3^+(v) + H_2 \longrightarrow H_3^+ + H_2^{*}. \tag{2}$$

An appreciation of these reactions facilitates the discussion of H_3^+ recombination given below. H_3^+ ions are important precursor ions in interstellar cloud ion chemistry; they are formed by reaction (1) following the production of H_2^+ by cosmic ray ionization of H_2. Hence a knowledge of the rate of recombination of H_3^+ ions in interstellar clouds is of great importance to the understanding of the physics and chemistry of interstellar clouds[7,8] (and similarly of the atmospheres of the outer planets[33]). Therefore a good deal of experimental effort has been expended in recent years to determine the recombination coefficient for H_3^+ ions.

Very early SA studies of $\alpha(H_3^+)$ in the 1950's gave conflicting results, although significantly (following the relatively recent FALP studies described below) one SA study by Persson and Brown[34] indicated that $\alpha(H_3^+)$ was small ($<3 \times 10^{-8} cm^3 s^{-1}$) at 300K. Subsequent SA studies at 300K by Leu et al[35] and Macdonald et al[36] indicated that $\alpha(H_3^+)$ was "typical" for most molecular ions at about $2 \times 10^{-7} cm^3 s^{-1}$, and this was given credence by the merged beam studies of Mitchell et al[37] who derived a similar $\alpha(H_3^+)$ for a temperature of 300K from their cross section data. Hence $\alpha(H_3^+)$ values of this magnitude were naturally invoked in models of the ion chemistry of interstellar clouds.

To study the recombination of H_3^+ ions using the FALP apparatus with the preferred helium carrier gas, a potential problem arises viz: He^+ ions react only very slowly with H_2[38]. Fortunately, however, H_2 reacts relatively rapidly with He_2^+ [39] and helium metastable atoms[40]. Therefore, it was important to ensure that the majority of the He^+ ions formed in the discharge were converted to He_2^+ by the three-body reaction of He^+ with two He atoms and this is the case at the normal helium operating pressures of 1 torr. On addition of H_2 to the afterglow (at a concentration of about one percent of the helium concentration), the He_2^+ ions were rapidly converted to HeH^+, He_2H^+ and H_2^+ ions and the metastables to H_2^+ ions and these product ions all react rapidly with H_2 to form H_3^+ ions[41]. Thus an afterglow plasma can be created at 300K consisting mainly of H_3^+ ions and electrons but with a small percentage

of He$^+$ ions as determined by the downstream mass spectrometer detection system. However, at the lower temperature of 95K at which recombination of H$_3^+$ ions was also studied, the three-body association reaction which converts He$^+$ to He$_2^+$ is much faster and the plasma flow velocity is much smaller so that the conversion of He$^+$ to He$_2^+$ is complete prior to the downstream reaction zone and no significant He$^+$ was observed in the plasma mass spectrum. (Interestingly, a small signal of He$_3^+$ was observed.) So on the addition of sufficient H$_2$ to the plasma an H$_3^+$/electron plasma was formed. On the addition of large flows of H$_2$ at 95K, H$_5^+$ appeared in the mass spectrum as a result of the three-body association reaction of H$_3^+$ with H$_2$ (with helium as a third-body). The appearance of H$_5^+$ correlated with a rapid reduction in the electron density in the afterglow plasma (indicating the onset of H$_5^+$ recombination with electrons).

Having created the H$_3^+$/electron plasma, the n_e was measured as a function of z using the movable Langmuir probe[41]. A typical result of the many data sets obtained at 300K is shown in Fig. 1 where it can be seen that following an initial relatively rapid reduction in n_e then the log n_e versus z plot is linear with a small slope which is indicative of slow diffusive loss of electrons. This plot should be compared with that also obtained at 300K for the O$_2^+$/electron plasma given in Fig. 1 from which an α(O$_2^+$) of 2×10^{-7}cm^{3}s^{-1} is derived. Clearly, the H$_3^+$/electron plasma is decaying principally by ambipolar diffusion and not recombination and certainly α(H$_3^+$)$<<\alpha$(O$_2^+$) = 2×10^{-7}cm^{3}s^{-1}. An analysis of the FALP data indicates that α(H$_3^+$) must be less than 2×10^{-8}cm^{3}s^{-1} at 300K and a similar upper limit value is also obtained at 95K. Similar results were obtained in a D$_3^+$/electron plasma. These values for α(H$_3^+$) are clearly in conflict with the values derived from both SA and merged beam experiments. However, after obtaining the FALP data and prior to its publication, we became aware of the theoretical work of Michels and Hobbs[42] which predicted that α(H$_3^+$) should be very small for ground vibrational state H$_3^+$ ions but appreciable for vibrationally-excited ions. This work not only supports the FALP results but also provides an explanation for the initial relatively rapid

reduction in n_e with z in the H_3^+/electron plasma. Since the H_3^+ ions are formed via reaction (1) then they are initially vibrationally excited and a fraction of them can recombine immediately after formation, although the majority will be relaxed in collisions with H_2 (i.e. via reaction (2)).

These FALP results prompted further SA afterglow experiments and it now appears that the SA values for $\alpha(H_3^+)$ were anomolously high due to impurities of CH_5^+ in the afterglows[26]. Since $\alpha(CH_5^+)$ is 1.1 × $10^{-6}cm^3s^{-1}$ at 300K only a small percentage of CH_5^+ is required as a contaminant ion to confuse the determination of $\alpha(H_3^+)$. Also, recent merged beam studies of $\sigma(H_3^+)$ have shown that the σ decreases markedly as the fraction of $H_3^+(\nu)$ in the ion beam is decreased, and an upper limit estimate of $\alpha(H_3^+)$ for $H_3^+(\nu\leq1)$ ions of about $1\times10^{-8}cm^3s^{-1}$ has been derived from the data[12], in agreement with the FALP data.

Subsequently, we have developed a method by which we can compare the rates of recombination of various ions in the FALP plasma by observing the relative mass spectrometer signals of those ions for greatly differing electron number densities, n_e, in the plasma (remembering that a large n_e enhances recombination and would therefore reveal ions that have significant recombination coefficients). We have found no measurable differences between the loss of He^+, HeH^+ and H_3^+ ions for very large changes in n_e and therefore conclude that $\alpha(H_3^+) \simeq \alpha(HeH^+) \simeq \alpha(He^+)$ within the limits of accuracy of measuring relative peak heights of the mass spectrometer signals.

What then is the actual value of $\alpha(H_3^+)$? If $\alpha(H_3^+)$ is equal to $\alpha(He^+)$ then at the low values of n_e at which three-body effects are insignificant (which is certainly the situation in interstellar gas clouds) then we may assume that He^+ can only radiatively recombine with electrons and that the the radiative recombination coefficient of He^+, $\alpha_r(He^+)$, at plasma temperature of 300K is $\leq 10^{-11}cm^3s^{-1}$ [1]. Presumably therefore $\alpha_r(H_3^+)$ will be similar. These α_r increases with decreasing temperature and will thus somewhat exceed $10^{-11}cm^3s^{-1}$ in cold interstellar clouds.

For large n_e and especially at low temperatures, the collisional-

radiative recombination process can occur. According to the published table[1], the collisional-radiative recombination coefficient, α_{cr}, for H^+ ions at a temperature of 250K and an n_e of $10^{10} cm^3 s^{-1}$, i.e. approximating to the physical conditions in the FALP plasma, is about $10^{-9} cm^3 s^{-1}$ (note that α_{cr} is not expected to depend significantly on the nature of the ion as long as it is singly-charged). At a fixed temperature, α_{cr} increases approximately linearly with n_e and thus at 250K and $10^{13} cm^{-3}$ then α_{cr} is about $10^{-6} cm^3 s^{-1}$. Clearly under such conditions the simple reciprocal density recombination law (i.e. $n_e^{-1} \propto z$) will not hold since it assumes that α is independent of n_e. This cannot be put to the test in the FALP since n_e in excess of a few times $10^{10} cm^{-3}$ cannot be attained. However, very recently, measurements have been made of the temporal decay of ground vibrational state H_3^+ ions in the afterglow of an electrical discharge through H_2 using an infrared absorption technique to detect and monitor the number density of ground state H_3^+ ions[43]. A value for $\alpha(H_3^+)$ of $1.8 \times 10^{-7} cm^3 s^{-1}$ at a temperature of about 210K was reported which again cast some doubt on the much lower value deduced from the FALP data. However, it must be said that this experiment involved a number of uncertainties which leads one to doubt the result. The electron density was not determined in this experiment and so n_e was equated to the ground state H_3^+ number density, and the likely presence of significant number densities of H^+ ions was ignored. Also the electron temperature was uncertain and could have been in excess of the gas temperature (rather than equal to the gas temperature as was assumed) in the very early ($\sim 10^{-3}$ to $10^{-4} s$) afterglow following a heavy current discharge through the H_2. The presence of $H_3^+(\nu)$ and also H_5^+, both of which are known to recombine rapidly with electrons, cannot be ruled out entirely, and the inevitable vibrational excitation and dissociation of the H_2 (generating reactive H atoms) introduces uncertainties into the ion chemistry which are difficult to quantify. So it seems possible that the loss rate of ground state H_3^+ ions from the plasma may be enhanced since they are coupled via the interaction processes to the rapidly recombining $H_3^+(\nu)$ and H_5^+. What seems even more likely is that, at the high n_e in the plasma ($\gtrsim 10^{13} cm^{-3}$), the collisional-radiative process mentioned above is

contributing to, and is probably the major loss process for H_3^+ ions. Under such circumstances, also noted above, a linear plot of the reciprocal number density of H_3^+ against time in the decaying afterglow would not be expected, yet this was apparently obtained and resulted in the large value of $\alpha(H_3^+)$. This is a perplexing situation. Clearly, further experiments are needed, if possible at much smaller n_e which would avoid many of the problems alluded to above. Meanwhile, the $\alpha(H_3^+)$ value derived from this experiment should be treated with some caution. This is surely not the last word on this problem !

DISSOCIATIVE RECOMBINATION OF PROTONATED MOLECULES

The addition of a wide variety of molecular gases, X, to an H_3^+/electron plasma initiates the proton transfer reactions:

$$H_3^+ + X \longrightarrow XH^+ + H_2 \qquad (3)$$

Such reactions are rapid, essentially occurring on each collision between H_3^+ and X, when the proton affinity (PA) of X exceeds $PA(H_2)$. This then provides the means of determining the α for many protonated molecules, i.e. XH^+ ions. Fig.1 shows the n_e versus z data obtained when CO and N_2 are added to an H_3^+/electron plasma in the FALP apparatus[41]. It clearly shows that HCO^+ and N_2H^+ plasmas decay more rapidly than H_3^+ plasmas, and it is also evident that $\alpha(N_2H^+) > \alpha(HCO^+)$ (the values are 1.7×10^{-7} and 1.1×10^{-7} in $cm^3 s^{-1}$ at 300K respectively). These α values were obtained from plots of n_e^{-1} versus z as mentioned previously. These measurements together with measurements at 95K indicated that $\alpha(N_2H^+)$ and $\alpha(HCO^+)$ varied approximately as T^{-1}. The larger recombination coefficients (e.g., $\alpha(CH_5^+)$) increased more slowly with decreasing temperature in accordance with the results of other studies for different ion species[27].

More recently, a FALP study of the α for several more protonated species has been carried out at 300K, varying in complexity from H_2F^+ to the clustered species $H^+(C_2H_5OH)_3$[44]. The results of this study revealed a trend of increasing α with increasing complexity of the recombining ion. Thus $\alpha(H_2F^+) = 1.1 \times 10^{-7} cm^3 s^{-1}$ and $\alpha(H^+(C_2H_5OH)_3) = 2 \times 10^{-6} cm^3 s^{-1}$, again a not unexpected result in the light of previous

studies[10]. These data find valuable application to the ion-chemical modelling of interstellar molecular clouds in which it is certain that many of these protonated molecules exist.

THE NEUTRAL PRODUCTS OF DISSOCIATIVE RECOMBINATION REACTIONS

It is obviously desirable to know the products of dissociative recombination reactions of polyatomic ions in order to obtain a better understanding of both the fundamentals of the reaction process and of the ion chemistry of real plasmas such as interstellar gas clouds. Theoretical effort has been directed to this problem with some conflicting results[1, 46-48]. Yet no experimental data are available relating to ground state polyatomic ions (although some information is available on the products of recombination of a few internally excited ionic species[13,45])). However, experiments are underway at the Universities of Birmingham, U.K. and Rennes, France to determine the products of dissociative recombination of some important interstellar species including H_3O^+, NH_4^+ and H_2CN^+ . To this end, vacuum ultraviolet (VUV) absorption spectroscopy (to detect atomic radicals such as H, O and N) and laser induced fluorescence (LIF) spectroscopy (to detect molecular radicals such as OH, NH and CN) are being used to probe recombining plasmas in FALP apparatuses.

Preliminary results have been obtained using the Birmingham FALP/LIF facility which indicate that OH radicals are generated in the dissociative recombination reaction of H_3O^+ with electrons. Although the experiment is not yet fully quantitative the time is not far off when the percentage of the recombination events which lead to OH radicals will be determined. Also, when the VUV absorption experiments at the Lyman α wavelength reveal the percentage of H atoms which are released following recombination, then a good deal will be known about the products of recombination of H_3O^+ ions.

REFERENCES

1) Bates, D.R. and Dalgarno, A., in "Atomic and Molecular Processes", Pure and Applied Physics Vol.13, Ed. D.R. Bates (Academic:New York, 1962); Bates, D.R., in "Recent Studies in Atomic and Molecular Processes", Ed. A.E. Kingston (Plenum:New York, 1987) p.1.

2) Bardsley, J.N. and Biondi, M.A., Adv. Atom. Mol. Phys. 6, 1 (1970).

3) Massey, H.S.W. and Gilbody, H.B., "Electronic and Ionic Impact Phenomena" Vol IV, (Clarendon:Oxford, 1974).

4) Mitchell, J.B.A., in "Atomic Processes in Electron-Ion and Ion-Ion Collisions", Ed. F. Brouillard (Plenum:New York, 1986)p. 185.

5) Thomas, L., Radio Sci. 9, 121 (1974).

6) Smith, D. and Adams, N.G., Topics in Current Chemistry 89, Plasma Chemistry I, 1 (1980).

7) Dalgarno, A. and Black, J.H., Rept. Prog. Phys. 39, 573 (1976).

8) Smith, D. and Adams, N.G., Int. Rev. Phys. Chem. 1, 271 (1981).

9) Smith, D. and Adams, N.G. in "Physics of Ion-Ion and Electron-Ion Collisions" Ed. F. Brouillard and J.W. McGowan (Plenum:New York, 1983) p.501.

10)Biondi, M.A., Comm. Atom. Mol. Phys. 4, 85 (1973).

11)Mitchell, J.B.A. and McGowan, J.W. in "Physics of Ion-Ion and Electron-Ion Collisions" Ed. F. Brouillard and J.W. McGowan (Plenum:New York, 1983)p. 279.

12)Hus, H., Youssif, F., Sen, A. and Mitchell, J.B.A., Proceedings 5th International Swarm Seminar, Birmingham, England 29-31 July 1987, p.82.

13)Adams, N.G. and Smith, D., in "Rate Coefficients in Astrochemistry" Ed. T.J. Millar and D.A. Williams (Reidel:Dordrecht, 1988) in press.

14)Smith, D., Dean, A.G. and Adams, N.G., Z.Physik 253, 191 (1972).

15)Adams, N.G., Dean, A.G. and Smith, D., Int. J. Mass Spectrom. Ion Phys. 10, 63 (1972/73).

16)Ferguson, E.E., Fehsenfeld, F.C. and Schmeltekopf, A.L., Adv. Atom. Mol. Phys. 5, 1 (1969).

17)Smith, D. and Adams, N.G., in "Gas Phase Ion Chemistry" Vol 1, Ed. M.T. Bowers (Academic:New York, 1979) p.1.

18)Ferguson, E.E., Fehsenfeld, F.C. and Albritton, D.L., in "Gas Phase Ion Chemistry" Vol 1, Ed. M.T. Bowers (Academic:New York, 1979) p.45.

19)Smith, D. and Adams, N.G., Adv. Atom. Mol. Phys. 24, (1988) in press.

20)Adams, N.G. and Smith, D., in "Techniques for the Study of Gas-Phase Ion-Molecule Reactions", Ed. J.M. Farrar and W.H. Saunders Jr. (Wiley-Interscience: New York, 1988) in press.

21)Smith, D. and Plumb I.C., J. Phys. D 5, 1226 (1972).

22)Smith, D., Adams, N.G., Dean, A.G. and Church, M.J., J.Phys. D. 8, 141 (1975).

23)Alge, E., Adams, N.G. and Smith, D., J. Phys. B 16, 1433 (1983).

24)Adams, N.G., Church, M.J. and Smith, D., J.Phys. D 8, 1409 (1975).

25)Walls, F.L. and Dunn G.H., J. Geophys. Res. 79, 1911 (1974).

26)Johnsen, R., Int. J. Mass Spectrom. Ion Processes 81, 67 (1987).

27)Smith, D. and Adams, N.G. in "Swarms of Ions and Electrons in Gases", Ed. W. Lindinger, T.D. Mark and F. Howorka, (Springer-Verlag:Vienna, 1984) p.284.

28)Huang, C-M., Biondi, M.A. and Johnsen, R., Phys. Rev. A14, 984 (1976).

29)Huang, C-M., Whitaker, M., Biondi, M.A. and Johnsen, R., Phys. Rev. A18, 64 (1978).

30)Leventhal, J.J. and Friedman, L., J. Chem. Phys. 50, 2928 (1969).

31)Bowers, M.T., Chesnavich, W.J. and Huntress, W.T. Jr., Int. J. Mass Spectrom. Ion Phys. 12, 357 (1973).

32)Kim, J.K., Theard, L.P. and Huntress, W.T. Jr., Int. J. Mass Spectrom Ion Phys. 15, 223 (1974).

33)Dalgarno, A., in "Rate Coefficients in Astrochemistry", Ed. T.J. Millar and D.A. Williams (Reidel:Dordrecht, 1988) in press.

34)Persson, K.B. and Brown S.C., Phys. Rev. 100, 729 (1955).

35)Leu, M.T., Biondi, M.A. and Johnsen, R., Phys. Rev. A8, 413 (1973).

36)Macdonald, J.A., Biondi, M.A. and Johnsen, R., "Planet. Space Sci.

$\underline{32}$, 651 (1984).

37)Mitchell, J.B.A., Ng, C.T., Forard, L., Janssen, R. and McGowan, J.W., J. Phys. B. $\underline{17}$, L909 (1984).

38)Johnsen, R. and Biondi, M.A., J. Chem. Phys. $\underline{61}$, 2127 (1974); $\underline{74}$, 6996 (1981).

39)Adams, N.G., Bohme, D.K. and Ferguson, E.E., J. Chem. Phys. $\underline{52}$, 5101 (1970).

40)Lindinger, W., Schmeltekopf, A.L. and Fehsenfeld, F.C., J. Chem. Phys. $\underline{61}$, 2890 (1974).

41)Adams, N.G., Smith, D. and Alge, E., J.Chem. Phys. $\underline{81}$, 1778 (1984).

42)Michels, H.H. and Hobbs, R.H. Ap. J. (Letters) $\underline{286}$, L27 (1984).

43)Amano, T., Ap. J. (Letters) submitted.

44)Adams, N.G. and Smith, D., Chem. Phys. Letts. $\underline{144}$, 11 (1988).

45)Smith, D., Phil. Trans. Roy. Soc. Lond. $\underline{A324}$, 257 (1988).

46)Herbst, E., Ap. J. $\underline{222}$, 508 (1978).

47)Bates, D.R., Ap. J. (Letters) $\underline{306}$, L45(1986).

48)Millar, T.J., DeFrees, D.J., McLean, A.D. and Herbst, E., Astron. Astrophys. $\underline{194}$, 250 (1988).

APPENDIX 5

DETERMINATION OF THE PROTON AFFINITIES OF H_2O AND CS_2

RELATIVE TO C_2H_4

B.J. McINTOSH, N.G. ADAMS and D. SMITH

DETERMINATION OF THE PROTON AFFINITIES
OF H₂O AND CS₂ RELATIVE TO C₂H₄

Bruce J. McINTOSH, Nigel G. ADAMS and David SMITH

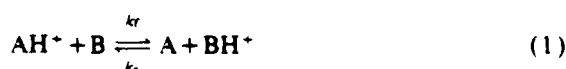*Department of Space Research, University of Birmingham, P.O. Box 363, Birmingham B15 2TT, UK*

The forward and reverse rate coefficients for the proton transfer reactions $C_2H_5^+ + H_2O \rightleftharpoons C_2H_4 + H_3O^+$, $C_2H_5^+ + CS_2 \rightleftharpoons C_2H_4 + CS_2H^+$ and $CS_2H^+ + H_2O \rightleftharpoons CS_2 + H_3O^+$ have been measured at 295 and 480 K and also at 210 K for the first of these reactions. Values of the enthalpy and entropy changes have been obtained from van 't Hoff plots. The entropy changes are found to be in excellent agreement with values calculated from ratios of rotational and translational partition functions. Using the proton affinity (PA) for C_2H_4 of 162.6 ± 0.5 kcal mol^{-1} as a reference, we obtain PA(H_2O) = 165.1 ± 0.7 and PA(CS_2) = 162.9 ± 0.7 kcal mol^{-1}.

1. Introduction

Much effort has been devoted over the past twenty years to the determination of proton affinities (PA) of a large number of atoms and molecules, as is evident from the extensive compilation of Lias, Liebman and Levin [1]. However, for many species there remains a lack of quantitative agreement between the PA values determined by different techniques.

The relative proton affinity of two bases A and B may be derived from a study of the proton transfer equilibrium

$$AH^+ + B \underset{k_r}{\overset{k_f}{\rightleftharpoons}} A + BH^+ \qquad (1)$$

by determining the equilibrium constant, K, and consequently the free energy change, $\Delta G^0 = -RT \ln K$ (although ΔH^0 is actually required; see below). K may be obtained by measurement of relative ion currents and neutral partial pressures using techniques such as pulsed electron beam high-pressure mass spectrometry (HPMS), flowing afterglow (FA), and ion cyclotron resonance (ICR) spectrometry. A potential problem is that the collection and detection efficiency of the different ion types may not be identical, and the measured ion current ratio, I_{BH^+}/I_{AH^+} requires correction for mass discrimination.

An alternative approach is to determine K ($= k_f/k_r$) from the ratio of the forward (k_f) and reverse (k_r) rate coefficients obtained from FA or selected ion flow tube (SIFT) experiments. This method circumvents the mass discrimination problem and by taking the ratio of the rate coefficients the effects of many of the systematic errors are eliminated. The principal limitation in determining K from k_f/k_r is that k_r becomes too slow to measure sufficiently accurately when $K \gtrsim 10^4$.

A complication that can arise in the higher-pressure experiments is that three-body association may be facile in the endothermic direction; examples of this process observed during the present study are discussed later. Clearly, the relative contributions of proton transfer and ternary association to a measured rate coefficient must be distinguished if meaningful results are to be derived.

Measurement of K provides only ΔG^0; in order to determine relative proton affinities (PA(A) − PA(B)) the enthalpy change for reaction (1), ΔH^0 ($= \Delta G^0 + T \Delta S^0$), is required. When the variation of K with temperature can be studied, then both ΔH^0 and the entropy change ΔS^0 for the reaction can be obtained directly from the slope and intercept, re-

142

spectively, of a van 't Hoff plot. Alternatively, ΔS^0 can be calculated by considering the partition functions of the reactants and products of the reaction. The rotational contribution is generally the most significant at thermal energies and may be estimated simply by using rotational symmetry numbers for reactions in which the geometries of the neutral and ion are similar. ΔS^0 may also be obtained from standard entropies; where these are unavailable (as is the case for many ions), standard entropies of isoelectronic neutrals can often be substituted without introducing serious errors.

The determination of *relative* proton affinities in the above manner provides a ladder of proton affinities. This ladder must be anchored at various points, however, by the assignment of *absolute* proton affinities as has recently been reviewed by McMahon [2]. The absolute proton affinity of any species (A) may be evaluated from standard heats of formation (ΔH_f^0) using the relationship

$$PA(A) = \Delta H_f^0(A) + \Delta H_f^0(H^+) - \Delta H_f^0(AH^+). \quad (2)$$

For most neutrals, $\Delta H_f^0(A)$ is readily available and since $\Delta H_f^0(H^+)$ is accurately known the problem reduces to the determination of $\Delta H_f^0(AH^+)$. The last mentioned may be evaluated from the ionization potential of AH where practicable or sometimes from the appearance potential of AH$^+$ from a larger molecule (or from a van der Waals cluster) [1,2]. Appearance potentials may be determined

experimentally from electron impact, photoionization or photoelectron–photoion coincidence (PEPICO) studies (mentioned in order of increasing accuracy and reliability [2]). For small molecules, ab initio calculations employing a sufficiently large basis set have been shown to yield absolute proton affinities of comparable accuracy to the most reliable experimental measurements [2]. Values for the heat of formation of $C_2H_5^+$ obtained from PEPICO and from photoionization experiments are in excellent agreement and the absolute proton affinity of C_2H_4 at 298 K is considered to be well established at 162.6 ± 0.5 kcal mol^{-1} [1,2]. Therefore we have selected this value for PA(C_2H_4) to obtain absolute values of PA(H_2O) and PA(CS_2) from our determinations of these PAs relative to C_2H_4.

The oxonium ion H_3O^+ plays an essential role in aqueous chemistry and biological processes and has recently been detected in interstellar clouds [3]. A reliable value of the absolute proton affinity of H_2O (and hence a value for $\Delta H_f^0(H_3O^+)$, see eq. (2)), would therefore find widespread application.

There have been several recent determinations (both relative and absolute) of the proton affinity of H_2O and these are compiled in table 1 and discussed later in this paper. All the previous relative measurements were made by obtaining ΔG^0 at a fixed temperature and ΔH^0 was then derived from this using a calculated value of ΔS^0 for
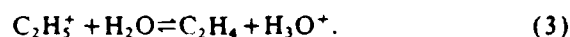
$$C_2H_5^+ + H_2O \rightleftharpoons C_2H_4 + H_3O^+. \quad (3)$$

Table 1

Recent determinations of the proton affinity of H_2O. Where a value of ΔS^0 for the reaction $C_2H_5^+ + H_2O \rightleftharpoons C_2H_4 + H_3O^+$ was required to convert the measured ΔG^0 to ΔH^0, the value used and the method of estimation are listed

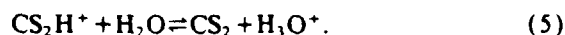| PA(H_2O) (kcal mol^{-1})	Method	Estimated ΔS^0 (cal mol^{-1} K^{-1})	Ref.
165.1 ± 0.7 [a]	this work (experimental ΔS^0)	-1.0	
164.8	ab initio calculation		[4]
165.1	ab initio calculation		[5]
165.3	ab initio calculation		[6]
166.5 ± 1.8 [b]	photoionization of (H_2O)$_2$		[7]
164.0 ± 1.7 [a]	k_f/k_r measured with SIFT		[8]
	(ΔS^0 from standard entropies)	$+2.3$	
166.7 [a]	ICR equilibria		[9]
	(ΔS^0 from symmetry number ratios)	-2.2	
166.4 ± 1.0 [a]	HPMS equilibria		[10]
	(ΔS^0 from standard entropies)	-1.2	

[a] Referenced to PA(C_2H_4) = 162.6 ± 0.5 kcal mol^{-1} [1,2].   [b] Corrected to 298 K [1].

We have studied this proton transfer reaction at 210, 295 and 480 K and determined $\Delta H^0(3)$ and $\Delta S^0(3)$ directly from a van 't Hoff plot. Reaction (3) has previously been investigated only at 298 K by Bohme and Mackay [8] using the SIFT technique.

Similarly, we have also determined the proton affinity of CS_2 relative to C_2H_4 from a study of the proton transfer reaction

$$C_2H_5^+ + CS_2 \rightleftharpoons C_2H_4 + CS_2H^+ \qquad (4)$$

and the proton affinity of H_2O relative to CS_2 from a study of the reaction

$$CS_2H^+ + H_2O \rightleftharpoons CS_2 + H_3O^+. \qquad (5)$$

The consistency of these measurements can be assessed using the relationship $\Delta H^0(3) = \Delta H^0(4) + \Delta H^0(5)$. It should be noted that reaction (5) has been studied previously by Meot-Ner and Field [11] using pulsed HPMS over the temperature range 370–570 K and these data are commented on below.

2. Experimental

The present work was carried out using the Birmingham variable-temperature SIFT apparatus [12,13]. The reactant ions were generated from ion–molecule reactions in a high-pressure electron impact ion source. H_3O^+ was produced from water vapour for the room-temperature and high-temperature studies. For the low-temperature measurements (to avoid condensation of water onto the ion entry orifice of the flow tube) a mixture of H_2 and CO was used, the H_3O^+ ions being formed here by a sequence of reactions starting with $O^+ + H_2$. $C_2H_5^+$ was produced from CH_4 and CS_2H^+ from a mixture of H_2 and CS_2 vapour. The reactant ions were injected into pure helium carrier gas and the reactant gases added downstream. The formation of the reactant ions by ion–molecule reactions in the ion source and the dissipation of any nascent vibrational excitation by multiple collisions with He in the flow tube ensured as far as possible that the reactant ions were in the ground state. When H_2O was the neutral reactant its relatively low vapour pressure necessitated the use of a 2% mixture of H_2O in He to facilitate the measurement of the H_2O flow rate.

Rate coefficients and product ion distributions

were determined in the usual manner for SIFT experiments [12,13]. Only inconsistent and irreproducible data could be obtained when using CS_2 as a neutral reactant at 210 K and this was attributed to condensation of CS_2 vapour onto the neutral inlet pipes and the flow tube wall.

3. Results

The forward and reverse rate coefficients were measured at 295 and 480 K for reactions (3), (4) and (5) and also at 210 K for reaction (3). The results are compiled in table 2 along with collisional rate coefficients calculated using the average dipole orientation (ADO) theory [14] for the polar reactant H_2O and the Langevin theory [14] for reactions involving CS_2 and C_2H_4 as the neutral reactants. An unreactive component was observed when studying the reactions of CS_2H^+ ($m/z = 77$ amu); this was attributed to the presence of $^{13}CS_2^+$ and $C^{32}S^{33}S^+$, which also have $m/z = 77$ amu.

Where ternary association and proton transfer occurred in parallel, the percentage proton transfer contribution to the total rate coefficient is noted in table 2. The association reaction of H_3O^+ and C_2H_4 will be discussed in detail in a forthcoming paper [15]. Where an association product was evident the flow tube pressure was varied in an attempt to resolve the measured total rate coefficient into binary (pressure independent) and ternary (pressure dependent) components. The non-linearity of the resulting plot of k versus pressure indicated that the association reaction was becoming saturated; that is, the rate of collisional stabilization of the association complex was comparable with the rate of its formation. The proportions of association and proton transfer were therefore determined solely from the product ion ratio at each pressure. To avoid mass discrimination the quadrupole mass spectrometer was operated at very low resolution and the product ion percentages are estimated to be correct to within ±3%.

The majority of the values of K are estimated to have uncertainties of ±10%, which correspond to uncertainties in $\ln K$ of ±0.1. For the 295 K values of $\ln K$ for reactions (3) and (4) these uncertainties are increased to ±0.2 due to an additional contri-

144

Table 2

Rate coefficients (in units of 10^{-10} cm^3 s^{-1}) and equilibrium constants for proton transfer reactions involving H_2O, C_2H_4 and CS_2 at the temperature T indicated. In some reactions, parallel proton transfer and association channels were evident and the rate coefficient for proton transfer given in this table has been taken as a percentage (given in parentheses) of the total rate coefficient for the overall reaction at a helium carrier gas pressure of 0.45 Torr

Reaction		$T = 210$ K	$T = 295$ K	$T = 480$ K	k_c [a]
$C_2H_5^+ + H_2O \rightleftharpoons H_3O^+ + C_2H_4$	k_f	20	18 [b]	12	19
	k_r	0.07 (10%)	0.4 [b] (40%)	1.3 (100%)	15
	K	290	45	9.2	
$C_2H_5^+ + CS_2 \rightleftharpoons CS_2H^+ + C_2H_4$	k_f		7.2	6.3	15
	k_r		0.45 (45%)	0.53 (100%)	11
	K		16	12	
$CS_2H^+ + H_2O \rightleftharpoons H_3O^+ + CS_2$	k_f		6.9	3.4	15
	k_r		2.5	6.0	11
	K		2.8	0.57	

[a] Collisional rate coefficient calculated using the ADO or Langevin theories [14] as appropriate.

[b] Bohme and Mackay [8] measured these rate coefficients as 14×10^{-10} and 0.63×10^{-10} cm^3 s^{-1}, respectively, giving $K = 22$.

bution from the uncertainty of the product ion ratio determination. For the 210 K value of ln K for reaction (3) this latter contribution increases the uncertainty to ± 0.3 since in this case the proton transfer rate is only $(10 \pm 3)\%$ of the total rate measured.
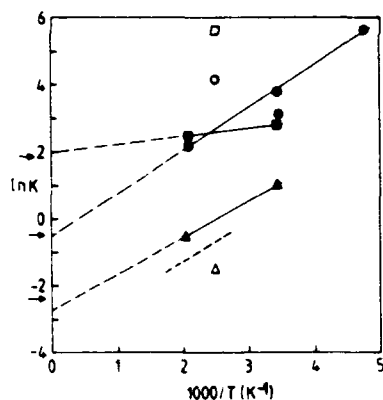

Fig. 1. Van 't Hoff plots for the reactions $C_2H_5^+ + H_2O \rightleftharpoons C_2H_4 + H_3O^+$ (3) (●); $C_2H_5^+ + CS_2 \rightleftharpoons C_2H_4 + CS_2H^+$ (4) (■) and $CS_2H^+ + H_2O \rightleftharpoons CS_2 + H_3O^+$ (5) (▲) constructed from the data given in table 2. The symbol (⊗) represents the SIFT measurement of Bohme and Mackay [8] for reaction (3) and the hollow symbols (○, □ and △ for reactions (3), (4) and (5), respectively) show values of K obtained from ΔG^0 values derived in the HPMS study of McMahon and Kebarle [10]. The dashed line represents data for equilibrium (5) from the HPMS study of Meot-Ner and Field [11]. The arrows along the y axis indicate calculated values of $\Delta S^0_{298}/R$.

Van 't Hoff plots of the data listed in table 2 are presented in fig. 1. These are based on the relationship

$$\ln K = \frac{\Delta S^0}{R} - \frac{\Delta H^0}{RT} \qquad (6)$$

which gives a linear plot if ΔH^0 and ΔS^0 do not change over the temperature range of the plot. When this is not true, values of ΔH^0_{298} and ΔS^0_{298} can be obtained by accounting for the temperature variation of ΔH^0 and ΔS^0 provided that the change in heat capacity at constant pressure (ΔC^0_p) is known, by use of the relationships

$$\Delta H^0_T = \Delta H^0_{298} + \int_{298}^{T} \Delta C^0_p \, dT, \qquad (7a)$$

$$\Delta S^0_T = \Delta S^0_{298} + \int_{298}^{T} \frac{\Delta C^0_p}{T'} \, dT. \qquad (7b)$$

Combination of eqs. (6), (7a) and (7b) then gives

$$\ln K + \frac{1}{RT} \int_{298}^{T} \Delta C^0_p \, dT - \frac{1}{R} \int_{298}^{T} \frac{\Delta C^0_p}{T'} \, dT$$

$$= \frac{\Delta S^0_{298}}{R} - \frac{\Delta H^0_{298}}{RT}. \qquad (8)$$

145

Table 3

Experimentally determined values of ΔH^0 (in kcal smol^{-1}) and ΔS^0 and calculated values of ΔS^0_{298} (in cal mol^{-1} K^{-1}) for proton transfer reactions involving C_2H_4, H_2O and CS_2

Reaction	ΔH^0 (exp.)	ΔS^0 (exp.)	ΔS^0_{298} (calc.)
(3) $C_2H_5^+ + H_2O \rightleftharpoons H_3O^+ + C_2H_4$	−2.5	−1.0	−1.0
(4) $C_2H_5^+ + CS_2 \rightleftharpoons CS_2H^+ + C_2H_4$	−0.45	4.0	3.7
(5) $CS_2H^+ + H_2O \rightleftharpoons H_3O^+ + CS_2$	−2.3	−5.5	−4.8

For the reactions discussed here, if it is assumed that for the rotational modes the classical and rigid rotor approximations are valid and that none of the vibrational modes are excited, then $\Delta C_p^0(3) = 0$, $\Delta C_p^0(4) = \frac{1}{2}R$ and $\Delta C_p^0(5) = -\frac{1}{2}R$. The heat capacity change in reactions (4) and (5) arises from the gain of a rotational degree of freedom in converting linear CS_2 to non-linear CS_2H^+. Insertion of these values into eq. (8) followed by integration gives

$$\ln K - \frac{1}{2}\left(\ln \frac{T}{298} + \frac{298}{T} - 1\right) = \frac{\Delta S^0_{298}}{R} - \frac{\Delta H^0_{298}}{RT}$$
(9)

for reaction (4) and a corresponding relationship for reaction (5) but with the sign of the term in parentheses on the left-hand side of eq. (9) reversed. For $T = 480$ K this correction term equals only 0.05, which is less than the experimental uncertainties in $\ln K$ estimated to be about ±0.1. Accordingly, no corrections have been made to the experimental $\ln K$ values and the values of ΔH^0 and ΔS^0 derived from the slopes and intercepts, respectively, of the van 't Hoff plots of fig. 1 are considered to be equal (within the estimated uncertainties) to ΔH^0_{298} and ΔS^0_{298}. These values of ΔH^0 and ΔS^0 are compiled together with calculated values of ΔS^0_{298} in table 3.

The calculated values of ΔS^0_{298} for reactions (3), (4) and (5) were obtained from the ratios of partition functions. Only the rotational and translational components were considered in the calculation, the former providing by far the most significant contribution in each reaction. Vibrational excitation was assumed to be unimportant over the temperature range employed. The rotational partition functions were computed using spectroscopic rotational constants for the neutral species [16] and from principal moments of inertia derived from optimized ab initio geometries for the ions. The lowest energy

structure for $C_2H_5^+$ is a C_{2v} non-classical bridged arrangement [17], H_3O^+ is pyramidal (C_{3v}) [4] and CS_2H^+ is non-linear (trans planar) [18]. The excellent agreement between the intercepts on the $\ln K$ axis of the van 't Hoff plots (fig. 1) and the calculated values of ΔS^0_{298} (arrows) indicates that neglect of vibrational excitation in the calculation of ΔS^0_{298} and in the assessment of the values of ΔC_p^0 is reasonable.

The value of $\Delta H^0(3)$ is considered the most reliable as it is derived from measurements taken over the widest temperature range. Using $PA(C_2H_4) = 162.6 \pm 0.5$ kcal mol^{-1} at 298 K, we therefore obtain $PA(H_2O) = 165.1 \pm 0.7$ kcal mol^{-1}. Combining this with $\Delta H^0_{f298}(H^+) = 367.19$ kcal mol^{-1} [19] and $\Delta H^0_{f298}(H_2O) = -57.796$ kcal mol^{-1} [19], eq. (2) gives $\Delta H^0_{f298}(H_3O^+) = 144.3 \pm 0.7$ kcal mol^{-1}. The enthalpy change in equilibrium (4) is then taken from the average of the measured $\Delta H^0(4)$ and $\Delta H^0(3) - \Delta H^0(5)$ to be -0.3 ± 0.2 kcal mol^{-1} giving $PA(CS_2) = 162.9 \pm 0.7$ kcal mol^{-1}. Using $\Delta H^0_{f298}(CS_2) = 27.98 \pm 0.19$ kcal mol^{-1} [19] then gives $\Delta H^0_{f298}(CS_2H^+) = 232.3 \pm 0.9$ kcal mol^{-1}.

Examination of table 1 reveals that the present value for $PA(H_2O)$ is in excellent agreement with three calculated ab initio values [4–6]. The result of Ng et al. [7] derived from the appearance potential of H_3O^+ from $(H_2O)_2$ also agrees with the present result within the large uncertainty of the Ng et al. measurement.
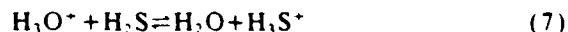
Bohme and Mackay [8] in a SIFT study at 298 K measured $K_3 = 22$ ($\Delta G^0(3) = -1.8$ kcal mol^{-1}) compared to our value of 45 ($\Delta G^0(3) = -2.3$ kcal mol^{-1}) at this temperature, this discrepancy being the net result of the lower value for k_3 and higher value for k_{-3} obtained by Bohme and Mackay compared to those obtained in the present study. Although the corresponding $\Delta G^0(3)$ values differ by

146

only 0.5 kcal mol^{-1}, Bohme and Mackay derived a value of $\Delta H^0(3) = -1.4$ kcal mol^{-1} using a value for ΔS^0 of $+2.3$ cal mol^{-1} K^{-1} estimated from standard entropies, and this contributes further to the disparity between their PA(H$_2$O) value and the present result.

The ICR equilibrium measurements of Collyer and McMahon [9] gave $\Delta H^0(3) = -4.1$ kcal mol^{-1} but in deriving this value $\Delta S^0(3)$ was overestimated as -2.2 cal mol^{-1} K^{-1}; use of our experimental value for $\Delta S^0(3)$ would reduce their value for $\Delta H^0(3)$ to -3.7 kcal mol^{-1}, which however, still remains significantly larger than our result. The recent pulsed electron beam HPMS study of McMahon and Kebarle [10] included both H$_2$O and CS$_2$ among compounds for which relative proton affinities were determined at 400 K. These data yield $\Delta H^0(3) = -3.8 \pm 0.5$ kcal mol^{-1} with $\Delta S^0(3)$ estimated from standard entropies to be -1.2 cal mol^{-1} K^{-1} (in close agreement with our experimental result). However, this value of $\Delta H^0(3)$ is unaccountably larger than our result. It should be noted that in both of these previous studies, equilibrium (3) could not be observed directly and the result quoted arises from summation of data for no less than three other equilibrium reactions.

For equilibrium (4) McMahon and Kebarle [10] obtained $\Delta H^0(4) = -3.5 \pm 0.5$ kcal mol^{-1} using an estimated $\Delta S^0(4)$ of 2.6 cal mol^{-1} K^{-1}; use of our calculated value at 400 K of 3.7 cal mol^{-1} K^{-1} reduces this to -3.0 kcal mol^{-1}, which is still in considerable conflict with our value of -0.6 ± 0.2 kcal mol^{-1}.

The temperature-variable pulsed HPMS experiment of Meot-Ner and Field [11] gave $\Delta H^0(5) = -2.3 \pm 0.4$ kcal mol^{-1} and $\Delta S^0(5) = -7.7 \pm 1.0$ cal mol^{-1} K^{-1}. This enthalpy change is in complete accordance with the present value although $\Delta S^0(5)$ deduced from the intercept of their van 't Hoff plot is more negative than the corresponding value obtained from the present data (see fig. 1). Meot-Ner and Field also studied the equilibrium

$$H_3O^+ + H_2S \rightleftharpoons H_2O + H_3S^+ \qquad (7)$$

over the temperature range 440–600 K and derived $\Delta H^0(7) = -5.0 \pm 0.4$ kcal mol^{-1}. Combining this with the recommended value [1] of 170.2 kcal mol^{-1} for the proton affinity of H$_2$S gives PA(H$_2$O) = 165.2

kcal mol^{-1}, which is in excellent agreement with our assignment.

4. Conclusions

We have determined PA(H$_2$O) = 165 1 $\pm$ 0.7 kcal mol^{-1} and PA(CS$_2$) = 162.9 $\pm$ 0.7 kcal mol^{-1} using PA(C$_2$H$_4$) = 162.6 $\pm$ 0.5 kcal mol^{-1}. Our value for PA(H$_2$O) differs significantly from previous determinations based on studies of proton transfer equilibria using HPMS and ICR techniques but agrees well with ab initio calculations. The excellent agreement between the present experimental value and the theoretical values further supports the assertion that ab initio calculations may be reliably employed to evaluate absolute proton affinities, at least for simple molecules such as H$_2$O. The credibility of our determinations is enhanced by their derivation from data obtained at more than one temperature and the requirement that two of the enthalpy changes measured should (and do within uncertainties) sum to equal the third.

Furthermore, values of ΔS^0 computed from partition functions (neglecting vibration) are in very good agreement with values derived from van 't Hoff plots. Thus, where the detailed structures of the reactant and product species are known, partition function calculations appear to provide reliable values of ΔS^0. The common practice of calculating ΔS^0 from rotational symmetry number ratios would provide particularly misleading results where a change from a linear to a non-linear structure occurs on protonation such as for CS$_2$ and CS$_2$H$^+$.

References

[1] S.G. Lias, J.F. Liebman and R.D. Levin, J. Phys. Chem. Ref. Data 13 (1984) 695.
[2] T.B. McMahon, in: Structure/reactivity and thermochemistry of ions, eds. P. Ausloos and S.G. Lias (Reidel, Dordrecht, 1987) p. 305.

147

[3] A. Wootten, F. Boulanger, M. Bogey, F. Combes, P.J. Encrenaz, M. Gerin and L. Ziurys, Astron. Astrophys. 166 (1986) L15.

[4] D.J. DeFrees and A.D. McLean, J. Comput. Chem. 7 (1986) 321.

[5] J.E. Del Bene, H.D. Mettee, M.J. Frisch, B.T. Luke and J.A. Pople, J. Phys. Chem. 87 (1983) 3279.

[6] J.A. Pople and L.A. Curtiss, J. Phys. Chem. 91 (1987) 155.

[7] C.Y. Ng, D.J. Trevor, P.W. Tiedemann, S.T. Ceyer, P.L. Kronebusch, B.H. Mahan and Y.T. Lee, J. Chem. Phys. 67 (1977) 4235.

[8] D.K. Bohme and G.I. Mackay, J. Am. Chem. Soc. 103 (1981) 2173.

[9] S.M. Collyer and T.B. McMahon, J. Phys. Chem. 87 (1983) 909.

[10] T.B. McMahon and P. Kebarle, J. Am. Chem. Soc. 107 (1985) 2612.

[11] M. Meot-Ner and F.H. Field, J. Chem. Phys. 66 (1977) 4527.

[12] N.G. Adams and D. Smith, Intern. J. Mass Spectrom. Ion Phys. 21 (1976) 349.

[13] D. Smith and N.G. Adams, in: Gas phase ion chemistry, Vol. 1, ed. M.T. Bowers (Academic Press, New York, 1979) p. 1.

[14] T. Su and M.T. Bowers, in: Gas phase ion chemistry, Vol. 1, ed. M.T. Bowers (Academic Press, New York, 1979) p. 83.

[15] N.G. Adams, D. Smith and B.J. McIntosh, to be published.

[16] G. Herzberg, Molecular spectra and molecular structure, Vol. 3. Electronic spectra and electronic structure of polyatomic molecules (Van Nostrand Reinhold, New York, 1967).

[17] R.Z. Liu and J.G. Yu, Intern. J. Quantum Chem. 23 (1983) 491.

[18] M. Scarlett and P.R. Taylor, Chem. Phys. 101 (1986) 17.

[19] D.R. Stull and H. Prophet, JANAF thermochemical tables, NSRDS-NBS 37 (1971).